THE ANALYSIS OF GRAVITY DATA OVER LAKE SUPERIOR TYPE IRON FORMATIONS

THESIS FOR THE DEGREE OF M.S.

MICHIGAN STATE UNIVERSITY RICHARD JOSEPH BLACKWELL 1964



LIBRARY
Michigan State
University

formations of
distorted by
This stud
methods which
sive use is ma
Four geol
theoretical gr
observed gravi
also available
Analysis of

of smooth curve

results compara

mation. Empiri

results to that

sound to be too

Talue. The meth

good results on

profile.

ABSTRACT

THE ANALYSIS OF GRAVITY DATA OVER LAKE SUPERIOR TYPE IRON FORMATIONS

by Richard Joseph Blackwell

The gravity anomalies associated with many of the iron formations of the Lake Superior region are often masked or distorted by regional gravity effects.

This study concerns itself with evaluating existing methods which remove or reduce the regional anomaly. Extensive use is made of digital computing and plotting equipment.

Four geologic cross-sections were selected and the theoretical gravity profiles were computed. Two profiles of observed gravity over areas containing iron formations were also available for study.

Analysis of the gravity profiles indicate that the method of smooth curves, combined with some geologic background yields results comparable to that of least squares polynomial approximation. Empirical grids were found to be equal in quality of results to that of the analytical grids. Both grid methods were found to be too powerful in their resolving power to be of optimum value. The method of downward continuation yielded consistently good results on both the theoretical and the observed gravity profile.

THE ANALYSIS OF GRAVITY DATA OVER LAKE SUPERIOR TYPE IRON FORMATIONS

Ву

Richard Joseph Blackwell

A THESIS

Submitted to
Michigan State University
in partial fulfillment of the requirements
for the degree of

MASTER OF SCIENCE

9 31501

The write

W. J. Hinze o

criticism dur

was formerly

University, c

to computer p

Jones and Lau

this study.

ACKNOWLEDGMENTS

The writer wishes to express his gratitude to Professor W. J. Hinze of Michigan State University, not only for suggesting this study, but for his patient and helpful guidance and criticism during the progress of the work. Marion Spohn, who was formerly with the Computer Laboratory at Michigan State University, offered many helpful suggestions and ideas related to computer programming. Special thanks are also due to the Jones and Laughlin Steel Corporation for providing data for this study.

Abstract .

Acknowledgm

List of Ill

List of Pla

I. Introduc

II. Criteria

III. Cross-se

A. Descr

1. ca

2. Ca

3. Ca

4. Ca

B. Depti

c. Obser

IV. Methods

V. Anomaly

A. smoot

B. Empir

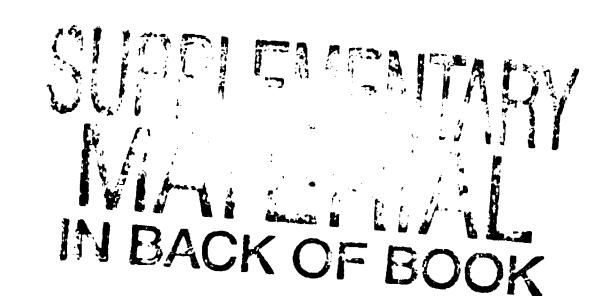


TABLE OF CONTENTS

Ab	str	act	-	•	• •	•	•	•	•	•	•	•	•	•	•	•	•	•	•	•	•	•	•	•	ii
Ac)	kno	wle	edg	me	nts		•	•		•	•	•	•	•	•	•	•	•	•	•	•	•	•	•	iii
Lis	st	of	I1	lu	str	at	io	ns			•	•	•	•	•	•	•	•	•	•	•	•	•	•	vii
Lis	st ·	of	Pl	at	es	•	•	•	•	•	•	•	•	•	•	•	•	•	•	•	•	•	•	•	×
I.	In	tro	du	ct	ion	١.	•	•	•	•	•	•	•	•	•	•	•	•	•	•	•	•	•	•	1
II.	Cr	it∈	eri	a i	Use	d	in	Se	ele	ect	tin	ng	Cr	08	ss-	-se	ect	tio	ons	5	•	•	•	•	3
III.	Cr	oss	;-s	ec	tio	ns	•	•	•	•	•	•	•	•	•	•	•	•	•	•	•	•	•	•	3
	A.	D∈	sc	rij	pti	.on	a	nd	Lo	oca	at:	ior	n:												
		1.	С	as	e I	• • .	Ama	asa	a (Οva	al	Aı	cea	a	•			•		•	•	•	•		4
		2.	С	as	e I	ī.	M	icl	niọ	gar	nme	e 1	10ı	ınt	tai	in	Aı	cea	a	•	•	•	•	•	5
		3.	С	as	e I	ΙI	. l	Maı	rqı	ıe†	tte	e I	Dis	stı	cio	ct	•	•	•	•	•	•	•	•	5
		4.	С	as	e I	v.	P	end	oke	ee-	-Go	oge	ebi	ĹС	Aı	cea	a	•	•	•	•	•	•	•	6
	в.	D∈	pt	h,	La	te	ra	1 1	Ext	ter	nt,	, ā	and	l f	Der	ns:	ity	Į	•	•	•	•	•		7
	c.	Ob	se	rv	ed	Gr	av:	ity	y I	Pro	of:	ile	es	•	•	•			•	•	•	•	•	•	8
ıv.	Me	the	ods	U	sed	li	n (Cor	npı	ut:	ing	g (Gra	av:	ity	, I	?ro	of:	il.	es	•	•	•		9
v.	An	oma	ıly	R	eso	lv	in	g!	Гес	chi	nic	que	es		•	•	•	•	•	•	•	•	•	•	20
	Α.	Sm	100	th	Co	nt	ou:	rs	•	•	•	•	•	•	•	•	•	•	•	•	•	•	•	•	21
	в.	En	iar	ri	cal	. G	ri	ds	•	•	•	•	•				•	•	•	•	•	•	•	•	21

C. 2nd De:

D. Least S

E. Downwa:

W. Interpret

A. Amasa (

1. Gene

2. 2nd

3. Smoo 4. Down

B. Michiga

1. Gene

2. _{2nd}

3. Smoc Poly

4. Down

C. Marquet

1. Gene

2. _{2nd}

3. Smoo

4. Dow:

	c.	2nd	Derivative Methods	•	•	•	•	24
	D.	Lea	ast Squares Polynomial Approximation	•	•	•		30
	E.	Dow	wnward Continuation Methods	•	•	•		35
VI.	In	terp	pretation of Results	•	•	•		37
	A.	Ama	asa Oval					
		1.	General Discussion	•	•	•	•	38
		2.	2nd Derivative and Empirical Grid .	•	•	•		39
		3.	Smooth Curves and Least Squares Polynomial Approximation	•		•	•	42
		4.	Downward Continuation	•	•	•		42
	в.	Mic	chigamme Mountain Area					
		1.	General Discussion	•	•	•		45
		2.	2nd Derivative and Empirical Grid .	•	•	•	•	46
		3.	Smooth Curves and Least Squares Polynomial Approximation	•	•	•	•	47
		4.	Downward Continuation	•	•	•	•	47
	c.	Mar	quette District					
		1.	General Discussion	•	•	•	•	50
		2.	2nd Derivative and Empirical Grid .	•	•	•	•	50
		3.	Smooth Curves and Least Squares Polynomial Approximation	•	•		•	51
		4.	Downward Continuation				_	54

	D.	Per	nokee-Gogebic
		1.	General Discussion
		2.	2nd Derivative and Empirical Grid 56
		3.	Smooth Curves and Least Squares Polynomial Approximation
		4.	Downward Continuation
VII.	Ob:	ser	ved Gravity Profile Interpretation 71
	A.	Mag	gnetic Center
		1.	General Discussion
		2.	Smooth Curves and Least Squares Polynomial Approximation
		3.	2nd Derivative and Empirical Grid 75
		4.	Downward Continuation
	в.	Bei	nding Lake
		1.	General Discussion
		2.	Smooth Curves and Least Squares Polynomial Approximation
		3.	2nd Derivative and Empirical Grid 82
		4.	Downward Continuation
vIII.	Co	ncl	usions
IX.	Re	com	mendations
v	p;	h];	ography 94

LIST OF ILLUSTRATIONS

Figure		Page
1.	Example of Lateral Extent	8
2.	Gravity Calculation Over Rectangular Prism	10
3.	Gravity Calculation Over Dipping Body	11
4.	Gravity Profile Construction	13
5.	Gravity Profile Construction	13
6.	Gravity Profile Construction	14
7.	Gravity Profile Construction	14
8.	Gravity Profile Construction	15
9.	Gravity Calculation Over N-sided Polygon	16
10.	Example of Smooth Curve Method	21
11.	Example of Empirical Grid	22
12.	Empirical Grid for Two Dimensions	23
13.	Example of Square Empirical Grid	24
14.	Example of 2nd Derivative Grid	28
15.	Example of Least Squares Transformation	31
16.	Example of Least Squares Transformation	31
17.	Amasa Oval Cross-section Smooth Curve	
	Least Squares Approximation	43
18.	Amasa Oval Cross-section 5-Point Downward Continuation	
	9-Point Downward Continuation	44

19.	Michigamme Mountain Cross-section Smooth Curve											
	Least Squares Approximation	•	•	•	48							
20.	Michigamme Mountain Cross-section											
	5-Point Downward Continuation											
	9-Point Downward Continuation	•	•	•	49							
21.	Marquette District Cross-section											
	Smooth Curve											
	Least Squares Approximation	•	•	•	52							
22.	Marquette District Cross-section											
	9-Point Downward Continuation	•	•	•	53							
23.	Penokee-Gogebic Cross-section											
	lst Degree Least Squares Approximation											
	2nd Degree Least Squares Approximation											
	3rd Degree Least Squares Approximation											
	4th Degree Least Squares Approximation	•	•	•	58							
24.	Penokee-Gogebic Cross-section											
	5th Degree Least Squares Approximation											
	6th Degree Least Squares Approximation	•	•	•	59							
25.	Penokee-Gogebic Cross-section											
	7th Degree Least Squares Approximation	•	•	•	60							
26.	Penokee-Gogebic Cross-section											
	8th Degree Least Squares Approximation	•	•	•	61							
27.	Penokee-Gogebic Cross-section											
	9th Degree Least Squares Approximation	•	•	•	62							
28.	Penokee-Gogebic Cross-section											
	Smooth Curve											
	10th Degree Least Squares Approximation	•	•	•	63							
29.	Penokee-Gogebic Cross-section (Vertical)											
	10th Degree Least Squares Approximation											
	9-Point Downward Continuation				64							

30.	Penokee-Gogebic Cross-section 18th Degree Least Squares Approximation	65
31.	Penokee-Gogebic Cross-section 9-Point Downward Continuation	70
32.	Magnetic Center Cross-section Smooth Curve 9th Degree Least Squares Approximation	74
33.	Magnetic Center Cross-section Rosenbach's 2nd Derivative Grid	77
34.	Magnetic Center Cross-section Elkins' I 2nd Derivative Grid	78
35.	Magnetic Center Cross-section Empirical Grid	79
36.	Magnetic Center Cross-section 9-Point Downward Continuation	80
37.	Bending Lake Cross-section Smooth Curve 7th Degree Least Squares Approximation	83
38.	Bending Lake Cross-section Rosenbach's 2nd Derivative Grid	83a
39.	Bending Lake Cross-section Elkins' 2nd Derivative Grid	84
40.	Bending Lake Cross-section Empirical Grid	86
41.	Bending Lake Cross-section 9-Point Downward Continuation	87

Plate

- I. Amasa
- II. Michie
- III. Marqu ϵ
- IV. Penoke

LIST OF PLATES

Plate

- I. Amasa Oval
- II. Michigamme Mountain
- III. Marquette District
 - IV. Penokee-Gogebic

of gravity date interesting at distorted by

One of

The ar

tions of the economically

on a regional is very diff:

potential mir

This same how the

A larg

of necessity
areas of rugg

support for h

Since most of

occur as long the anomalies

direction is,

this assumpti

INTRODUCTION

One of the most difficult problems in the analysis of gravity data is the accurate resolution of geologically interesting anomalies. These anomalies are often masked or distorted by regional effects.

The anomalies associated with many of the iron formations of the Lake Superior region exhibit this effect. The economically interesting anomaly is frequently superimposed on a regional anomaly having such a steep gradient that it is very difficult to isolate the anomaly associated with a potential mineral deposit.

This survey has been undertaken specifically to determine how the regional effect can best be removed or isolated.

A large number of the gravity surveys undertaken to locate mineral deposits are of a profile or line type. This is out of necessity because these surveys generally are located in areas of rugged topography or swamps. In addition, financial support for blanket coverage of an area is difficult to obtain. Since most of the iron formations of the Lake Superior region occur as long, linear, dipping formations, the assumption that the anomalies and their source are infinite in their strike direction is, therefore, a reasonable one. It is apparent that this assumption restricts this study to a two-dimensional form.

In order to gain some insight into the problem, the gravity profiles were computed theoretically for geologic cross-sections containing iron formations. Four cross-sections were selected from areas where the geology was known and where iron formations were present in various attitudes. The gravitational attraction over these sections was then computed, using the stratigraphic sequence occurring in that section.

Two additional profiles using actual observed gravity data were also available for study.

The six profiles, four theoretically computed and two observed, were analyzed with the following methods for isolation or removal of the regional anomaly: Smooth curving, the 2nd derivative methods using empirical and analytical grids, downward continuation, and least squares polynomial approximation.

All computations were carried out on a Control Data

Corporation 160A computer utilizing Fortran computer language.

Many of the results were plotted graphically on a digital incremental plotter connected to the computer.

The programming was carried out in such a manner that the results of one program would be punched on computer cards.

These same cards were later used in programs written to analyze the data.

Without the aid of a digital computer, a study of this kind would not have been feasible.

CRITERIA USED IN SELECTING CROSS-SECTIONS

The following conditions were given consideration during the selection of the geologic cross-sections:

- 1. Geologic information.
 - a) structure.
 - b) lithology.
 - c) attitude.
 - d) previous study in the area.
 - e) availability of geologic information.
- 2. Geophysical parameters.
 - a) density determinations.
 - b) steep regional gradients.
 - c) method of computing the gravity.
 - d) profile length and station spacing.

CROSS-SECTIONS

Four cross-sections were selected as being representative of the problem and fulfilling, in part, the geologic and geophysical requirements. The computed gravity profiles are all different in shape and amplitude. The resulting curves vary considerably in complexity and it is felt that

each curve has tested the usefulness of the methods available to remove or isolate the regional anomaly.

Description and Location

Case I. Amasa oval area. Plate I illustrates the crosssection and the formations that make it up. Shown on the plate are the individual anomalies associated with each formation and the composite curve across the section.

The Fence River formation represents an ideal case of an isolated, dipping unit enclosed by more massive formations.

The section cuts east-west through section 13 to section 17, T44N, R31W and is located just north of the east branch of the Michigamme Reservoir.

From east to west, the Michigamme slate, the Fence River formation, the Hemlock formation, the Randville dolomite and the Margeson Creek gneiss all dip about 60° to the east away from the center of the Amasa oval.

The Fence River formation in its upper half is a massive garnet-grunerite schist, while its lower westward half contains quartz, magnetite, hornblende, and epidote.

The cross-section is profile A-A' from Plate I of Gair's (1956) report.

Case II. Michigamme Mountain area. Plate II shows the irregular-shaped Goodrich quartzite with the more massive Randville dolomite and the Hemlock formation on each side. The anomalies associated with each formation are shown as is the composite gravity curve across the section.

The section lies about 3/4 mile north of the road junction known as Kiernan, Michigan and cuts east-west from the NE 1/4 of the SW 1/4 of section 3 to the NW 1/4 of the SE 1/4 of section 4, T43N, R31W in Iron County, Michigan.

The Goodrich quartzite is a magnetic cherty quartzite with much clastic quartz. Jaspilite and oblitic iron formations occur in pebble size and the iron content is estimated to be between 15% and 35% (Gair, 1956).

This section represents profile F-F', Plate III from Gair's (1956) report.

Case III. Marquette district. Plate III shows the cross-section of the geology found west of Ishpeming, Michigan and includes the Negaunee iron formation.

The cross-section is located several miles west of Ishpeming, and runs north-south through sections 30, 31, 6, 7, 18, and 19 of T47N, R27W.

An alternating series of peridotite-serpentinite sills and the Kitchi schist form a major portion of the cross-section while the Ajibic quartzite, Siamo slate, Negaunee iron formation, and the Michigamme slates make up the southern end of the cross-section.

The section was computed with all formations vertical in attitude. No accurate determination of attitude could be made for all the formations present. The southern end of the cross-section probably dips from 75° to 90° to the south.

Data for this section was taken from Van Hise' (1897) report.

Case IV. Penokee-Gogebic area. Plate IV shows the formations which make up this section. The geology is relatively simple, consisting of an iron formation made up of four separate units. The computed gravity profiles combine to give an anomaly that is indicative of the whole section.

This cross-section is located in the vicinity of Ironwood, Michigan. The section extends north-west to south-east through sections 6, 7, 18, 19, and 30 of T46N, R46W.

The Ironwood formation consists of: (1) Cherty iron-bearing slates and carbonates, (2) Ferruginous slates, (3) Ferruginous

cherts, and (4) Jaspilites and ore. This series is overlain by the massive Tyler slates to the north, and stratigraphically below the Ironwood formation is a granite and granite gneiss of large areal extent.

The Ironwood formation dips 60° to 65° to the northwest. This section was taken from Van Hise (1897).

Depth, Lateral Extent, and Density

In the computation of the gravity values over these profiles assumptions were made in regard to depth, lateral extent, and density.

Depths were taken from the maps of those areas where cross-sections were available, and in those areas where they were not available, the literature was searched for aid in making a judicious choice.

Lateral extent of the formations at each end of the cross-section plays an important role in the amplitude and gradient of the gravity anomaly. They are, in fact, the predominant source of the regional effect in computed gravity anomalies. End members were computed with widths of 200,000 feet, as shown in Figure 1 on page 8.

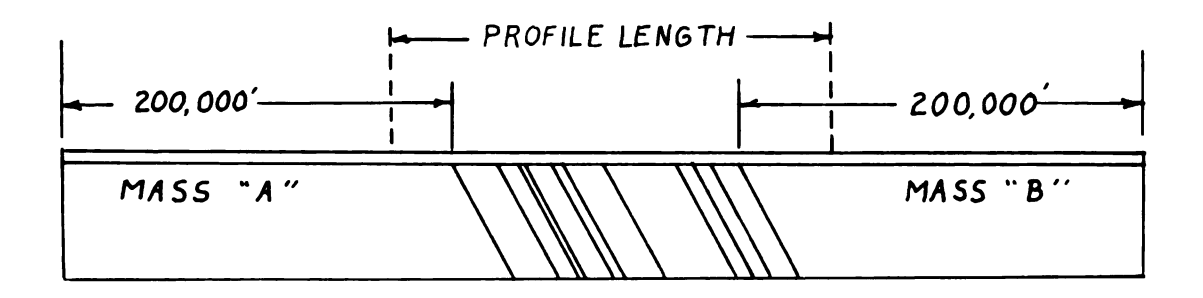


Figure 1

The selection of iron formation densities were made with the aid of a graph (Hinze, 1960) showing percent soluble iron (by weight) versus the density in grams per cubic centimeter for hematite and quartz rock, magnetite and quartz rock, and magnetite-quartz and garnet rock. In addition, Hinze (1963) and Jakosky (1950) also served as sources of information for the densities of the other rock formation.

Observed Gravity Profiles

In addition to the four cross-sections over which the gravity was computed, two profiles of observed gravity over known and located iron formations were available for study. Both exhibit very steep gradients with a residual anomaly superimposed in such a manner that accurate resolution is difficult.

METHODS USED IN COMPUTING GRAVITY PROFILES

It has been shown by Heiland (1940) that the vertical component of gravity for a two-dimensional body derives from a logarithmic potential, that is, the gravitational attraction is proportional to the disturbing formations section in a plane perpendicular to the strike of the body.

To determine the expression for a two-dimensional body, the volume integral (representing Newtonian potential)

$$U = 46 \iiint dx dy dz , \qquad (1)$$

is integrated from + (plus) to - (minus) infinity in the y-direction and the surface integral representing logarithmic potential is obtained,

$$U = 2 6 \int \int Log_2 dx dz , \qquad (2)$$

where

U = gravitational potential,

k = gravitational constant,

 δ = density,

r = distance from point of observation to the center of the disturbing mass,

dxdz = cross-sectional element.

By differentiating U with respect to z, equation (2)

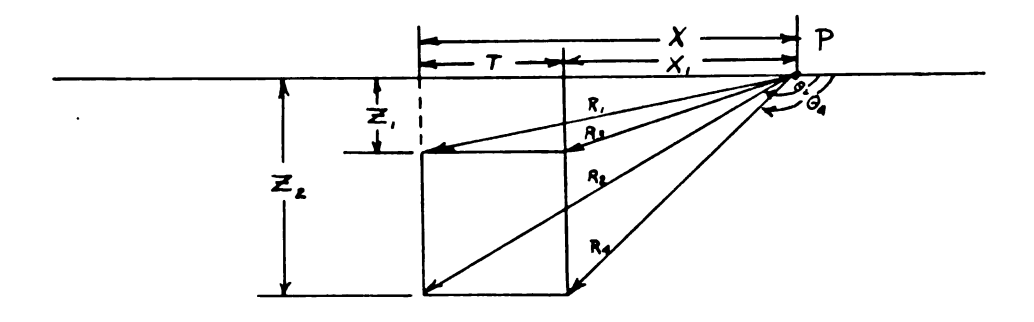
becomes

$$\Delta g = \frac{\partial U}{\partial Z} = 2 16 \iint \frac{Z}{\Lambda^2} dx dz , \qquad (3)$$

$$\Delta g = \text{gravity anomaly.}$$

where

If we wish to calculate the gravity anomaly at point P due to the rectangular block illustrated in Figure 2,



$$X - X_1 = T$$
 $Z_1^2 + X_2^2 = R_2^2$
 $Z_2^2 + X_3^2 = R_2^2$
 $Z_3^2 + (X - T)^2 = R_3^2$
 $Z_3^2 + (X - T)^2 = R_4^2$

$$X = Z_1 TAN \Theta_1$$

 $X = Z_2 TAN \Theta_2$
 $X - T = Z_1 TAN \Theta_3$
 $X - T = Z_2 TAN \Theta_4$

Figure 2

Using the above values and by integration, equation (3) becomes,

$$\Delta g = \int_{0}^{\tau} \int_{Z_{1}}^{Z_{2}} \frac{Z \, dx \, dZ}{Z^{2} + (X - X_{1})^{2}} , \qquad (4)$$

$$\Delta g = \int_{0}^{T} \log_{R} \sqrt{\frac{Z_{s}^{2} + (x - X_{s})^{2}}{Z_{s}^{2} + (x - X_{s})^{2}}} \, dx , \qquad (5)$$

$$\Delta g = 2k6 \left[x \log_2 \sqrt{\frac{Z_2^2 + X^2}{Z_1^2 + X^2}} - (X - T) \log_2 \sqrt{\frac{Z_2^2 + (X - T)^2}{Z_1^2 + (X - T)^2}} \right]$$
 (6)

$$+Z_{z}\left(TAN^{-1}\frac{X}{Z_{z}}-TAN^{-1}\frac{X-T}{Z_{z}}\right)+Z_{z}\left(TAN^{-1}\frac{X}{Z_{z}}-TAN^{-1}\frac{X-T}{Z_{z}}\right)$$

Equation (6) reduces to:

$$\Delta_{g} = 216 \left[\times LOG_{2} \frac{R_{2}R_{3}}{R_{1}R_{4}} + TLOG_{2} \frac{R_{4}}{R_{3}} + Z_{2} (\Theta_{2} - \Theta_{4}) - Z_{1} (\Theta_{1} - \Theta_{5}) \right]. (7)$$

Referring to Figure 3 which illustrates the notation used for dipping bodies, the expression for computing the gravity anomaly is given by equation (8),

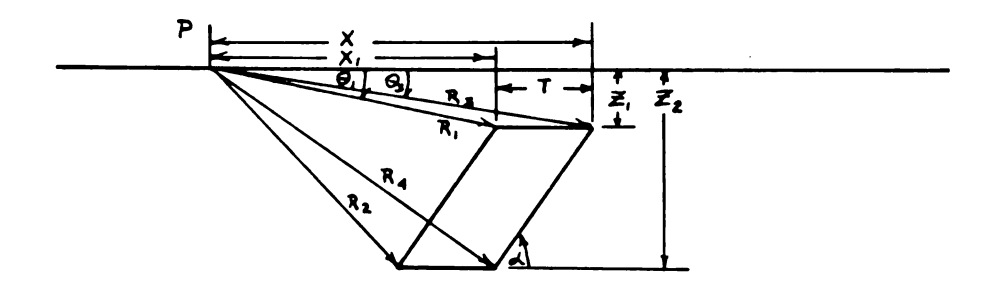


Figure 3

$$\Delta g = 2R6 - \left[X SIN_{x} + Z_{1} COS_{x} \right] SIN_{x} LOG_{x} \frac{R_{2}R_{3}}{R_{1}R_{4}} + COS_{x} \left(O_{2} - O_{1} \right)$$

$$+(\Theta-\Theta)$$
 + T SINZ SINZ LOG $\frac{R_1}{R_3}$ + COSZ($\Theta_4-\Theta_5$) + $Z_2(\Theta_2-\Theta_4)-Z_1(\Theta_1-\Theta_5)$. (8)

It is obvious that both equations (7) and (8) are long and would become exceedingly tedious to calculate by non-computer techniques if a great number of gravity values were needed. However, both equations, when broken down into smaller operations and the computations arranged in an orderly manner, lend themselves readily to computer programming.

It should be noted that the equations (7) and (8), while very accurate and easy to put in Fortran language, are in some respects limited in their use and adaptability. It was found that it takes approximately 4.5 to 5.0 seconds to evaluate one point using the Control Data 160A. Thus, if it were desired to compute 100 points on a profile over a single formation, it would take about 7.5 to 8.3 minutes. As in the case of the Marquette profile which consisted of 12 separate formations, each of which required 88 points at which the gravity was to be computed, the time required was $(12) \times (88) \times (5.0) = 5,280$ seconds or about one hour and 28 minutes to compute.

It should also be noted that in all equations concerned with gravity anomalies of bodies with high or low densities, the difference between the density of a body with density δ_1 and that of a surrounding formation of density δ_2 , must be substituted in place of the absolute density, therefore;

$$6 = 6, -6, .$$

The manner in which the gravity profiles were constructed from the geologic cross-sections is as follows: Given a formation of some dimensions and with a density of, let us say, 2.85, we wish to compute the gravity anomaly at a series of points in

a profile over this body that is enclosed on both sides by a mass of density, 2.70. This is illustrated in Figure 4.

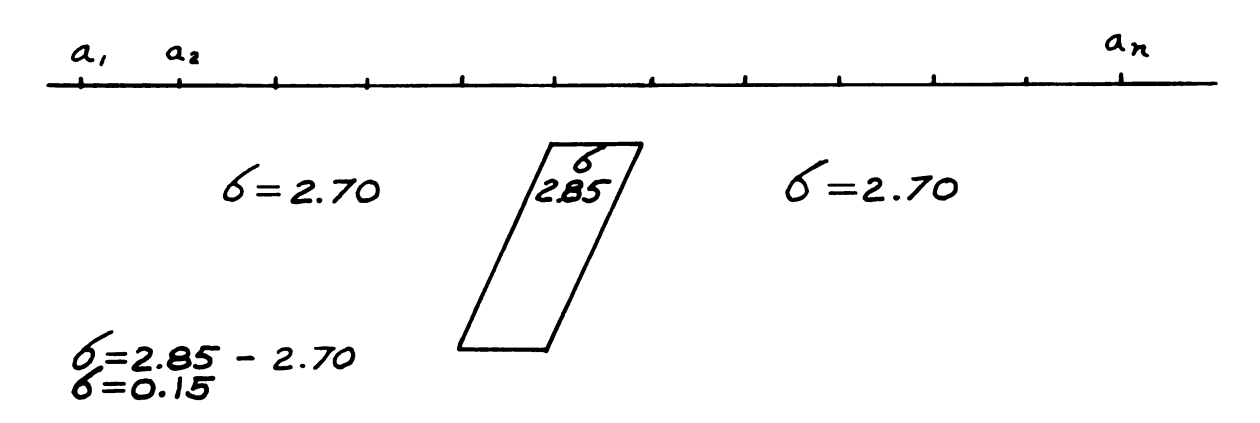


Figure 4

Proceeding with the computation, a series of points are plotted along a profile over the disturbing mass. The profile may look something like that shown in Figure 5.

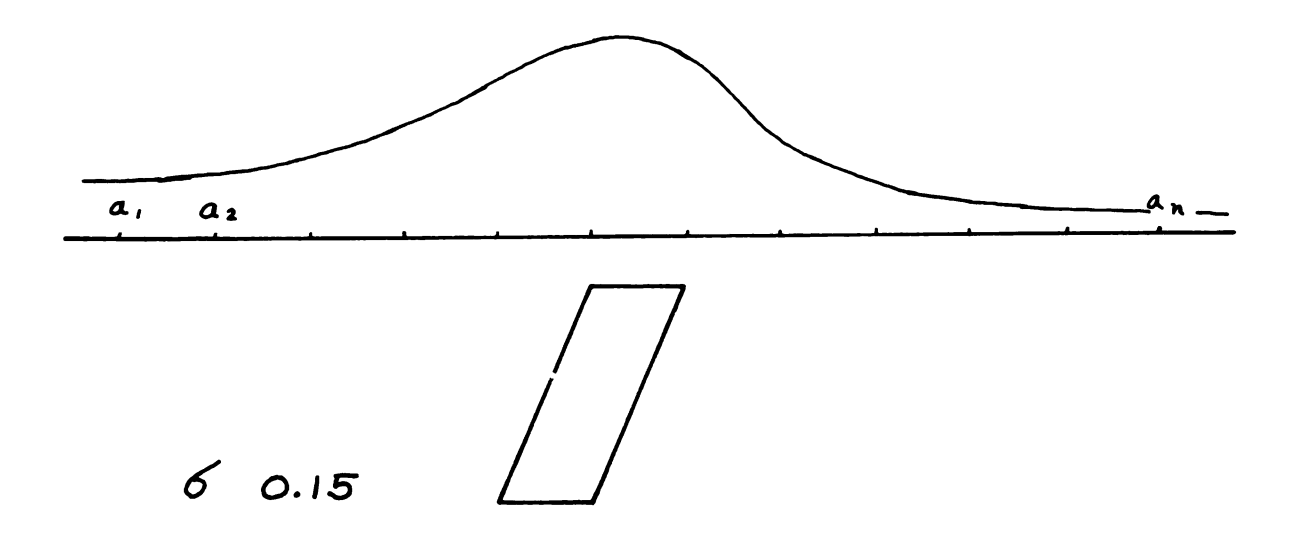


Figure 5

Next suppose we wish to compute the gravity anomaly of another body adjacent to body A, but with higher density, let us say, 3.20, and also surrounded by a mass of density 2.70, therefore:

$$6 = 3.20 - 2.70$$

 $6 = 0.50$

Suppose also that we wish to compute the anomaly of body B at exactly the same positions at which we computed body A's anomaly (Figure 6).

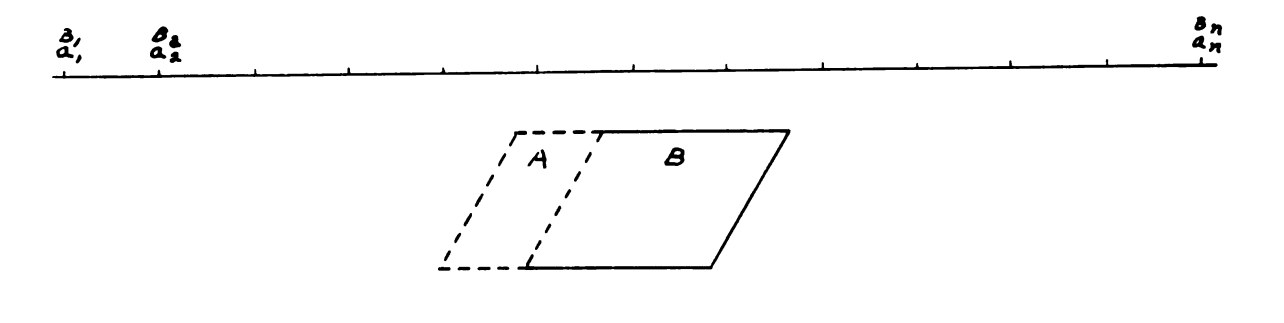


Figure 6

The second profile may look like that shown in Figure 7.

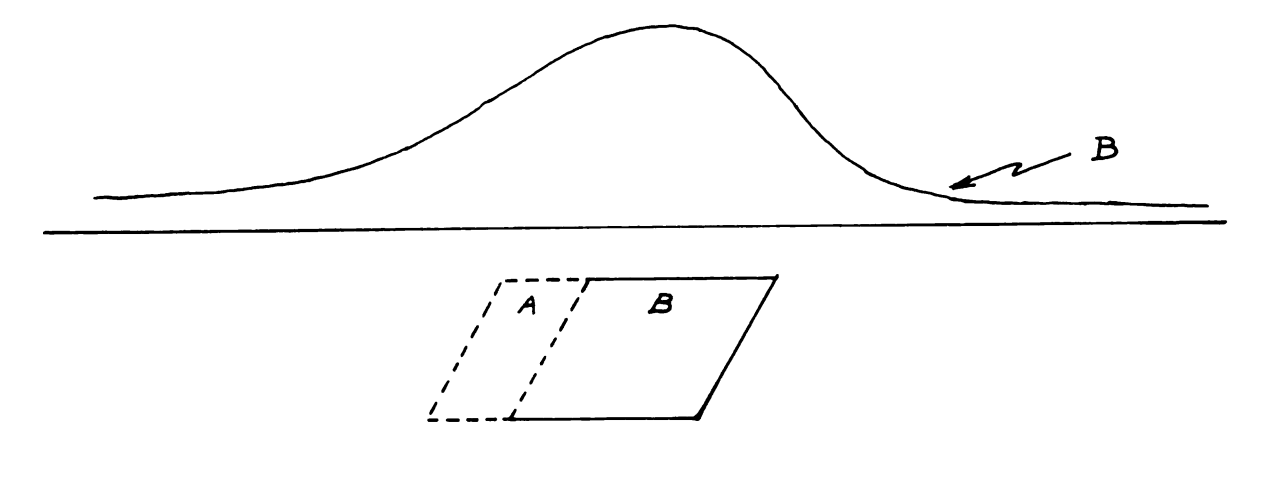


Figure 7

By combining the values of the anomaly shown in Figure 5 and the values as shown in Figure 7, a composite profile over the two masses is obtained. This is illustrated in Figure 8.

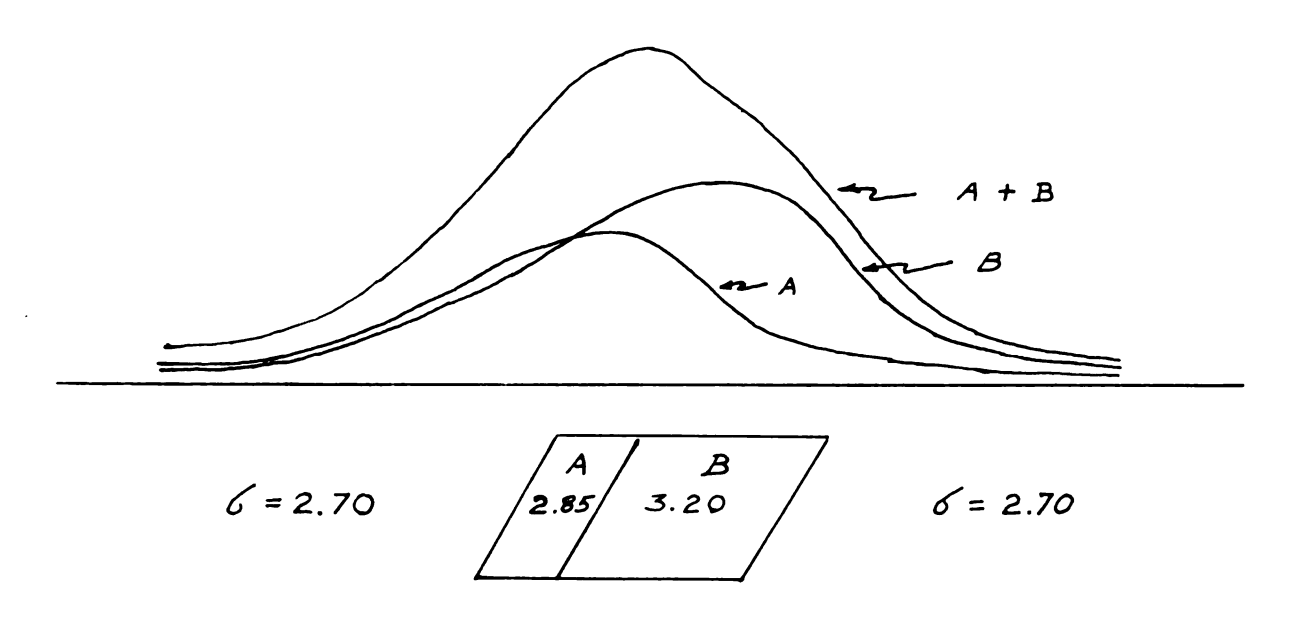


Figure 8

In this manner a profile for each individual formation was computed and then combined to give a total gravity anomaly over a geologic section.

In addition to the method used by Heiland and others to compute the gravitational effects of two-dimensional bodies, it is possible to use a method in which the disturbing body is represented by an N-sided polygon (Talwani, 1959). The method is highly successful and very adaptable to a study of this type.

The periphery of any two-dimensional body can be approximated by a polygon by making the number of sides sufficiently large. Analytical expressions can be obtained for the vertical component of gravity due to this polygon at any given point. The computation, while being lengthy and time-consuming, is largely repetitious and can be programmed for a digital computer.

Hubbert (1948) has shown that the vertical component of gravitational attraction due to a two-dimensional body is, at the origin of an xz coordinate system as shown in Figure 9, equal to:

$$\Delta g = 2 k \mathcal{O} \phi Z \mathcal{A} \theta , \qquad (9)$$

where z is defined to be positive downward (vertical) and θ is measured from the positive x-axis to the positive z-axis.

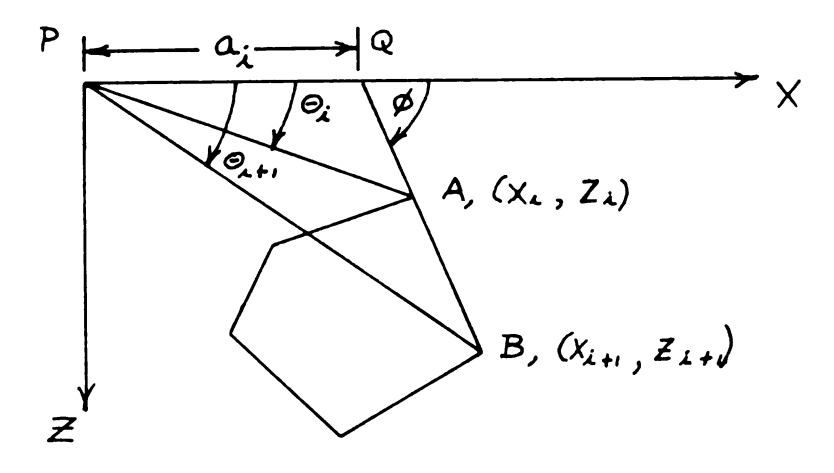


Figure 9

If the line integral is taken along the periphery of the body, the requirement will be to evaluate each side of the N-sided polygon.

For example, if we wish first to compute the contribution from side AB, referring to Figure 9, extend the side AB to meet the x-axis at Q at an angle \emptyset . By letting PQ = a_i ,

$$Z = (X - Q_{\perp}) TAN \emptyset$$
 , (10)

and for any arbitrary point R,

$$\mathbf{z} = \mathbf{x} \mathsf{TAN} \Theta , \qquad (11)$$

from equations (10) and (11) it can be shown that

$$Z = \frac{\text{Ai TAN } \Theta \text{ TAN } \Theta \text{i}}{\text{TAN } \Theta \text{i} - \text{TAN } \Theta} , \qquad (12)$$

or letting Δ $\mathbf{Z}_{\mathbf{i}}$ represent the gravity contributed by side AB

$$\Delta Z := \int_{a}^{b} Z d\theta = \int_{a}^{b} \frac{\Delta i \quad TAN\Theta \ TAN\Theta i}{TANØ - TANØ i} d\Theta . \quad (13)$$

By integrating equation (13) an expression is available for computation of each side of the polygon, that is:

$$\Delta Z_{i} = \alpha_{i} SIN \emptyset_{i} COS \emptyset_{i} \left[\Theta_{i} - \Theta_{i+1} + TAN \emptyset_{i} LOG_{a} \frac{COS \Theta_{i} (TAN \Theta_{i} - TAN \emptyset_{i})}{COS \Theta_{i+1} (TAN \Theta_{i+1} - TAN \emptyset_{i})} \right], (14)$$

where: $\Theta_{L} = ARCTAN \frac{ZL}{XL}$, (15)

$$\Theta_{i+1} = ARCTAN \frac{Z_{i+1}}{X_{i+1}} , \qquad (16)$$

$$\emptyset i = ARCTAN \frac{Z_{i+1} - Z_{i}}{X_{i+1} - X_{i}} , \qquad (17)$$

$$a_{\lambda} = \chi_{\lambda+1} + \chi_{\lambda+1} - \chi_{\lambda} \qquad (18)$$

and the gravity anomaly at P due to the N-sided polygon will be:

$$\Delta g = 2k\delta \sum \Delta Z_{i} \quad . \tag{19}$$

Equation (14) reduces to a simpler expression if the following conditions exist:

If
$$X_i = 0$$
,

$$\Delta Z_{i} = -\alpha_{i} SIN \phi_{i} COS \phi_{i} \left[\Theta_{i+1} - \frac{\pi}{2} + TAN \phi_{i} LOG_{e} \left(\cos \varphi_{i} (TAN \varphi_{i} - TAN \phi_{i}) \right) \right] (20)$$

If
$$X_{4+1} = 0$$
,

$$\Delta Z_{i} = Q_{i} SIN \phi_{i} cos \phi_{i} \left[\Theta_{a}, -\frac{\pi}{2} + TAN \phi_{i} LO G_{a} (cos \theta_{a} (TAN \theta_{i} - TAN \phi_{i})) \right] (21)$$

If Zi = Zi+, ,

$$\Delta Z_{i} = Z_{i} \left(\Theta_{i+1} - \Theta_{i} \right). \tag{22}$$

If $X_{i} = X_{i+1}$,

$$\Delta Z_{i} = X_{i} LOG_{a} \frac{COSO_{i}}{COSO_{i+1}}. \tag{23}$$

And if

$$Xi = Zi = 0$$
.

$$Xi_{i+1} = Zi_{i+1} = 0$$
.

 $\Theta i = \Theta i + i$

$$\Delta Z_{\lambda} = 0. \tag{24}$$

Since θ_i , θ_{i+1} , \emptyset_i and A_i can all be expressed in terms of x and z, and the expression which yields the gravity for a side of the polygon is given in explicit terms of θ_i , θ_{i+1} , \emptyset_i , and A_i or in trigonometric functions involving these terms the computations become arithmetic.

To use the method it is only required that the body be approximated with a polygon of N-sides, and that each side of the polygon be defined by a set of coordinates (x_i, z_i) and (x_{i+1}, z_{i+1}) which locate the two end points of the side.

Once the computer program is written to use Talwani's method, the only requirement is to put the coordinates of each side of the polygon on computer cards and determine where it is desired to start the profile and the number of computation points desired.

This method also was programmed but utilized only to check with the values determined with Heiland's method. Computation time is approximately equal to 2.0 (N) seconds.

(N = number of sides.) While the method is not fast, the restriction of having to have parallel sides is removed and the gravity of any shaped body can be computed.

The method was tested in Case II, the Michigamme Mountain section. Talwani's method was used with 15 sides to compute the gravity over the irregular-shaped Goodrich quartzite mass.

The correspondence with Heiland's results was not good.

Talwani's method was used again, but this time with 35 sides and the similarity with Heiland's method was within + 0.01 mgal. These results and methods will be discussed later under the evaluation of each profile.

In addition, cónsiderable time was saved by using Talwani's method. Heiland's formula for computing the gravity over a dipping tabular body was used to approximate the Goodrich quartzite. The cross-section of the body was approximated by using 30 tabular bodies, each 30 feet wide. Each of the 30 bodies required 70 points at which the gravity was to be calculated. This means that 2,100 calculations were required to arrive at a total gravity profile over the mass. The time required was about two hours and 15 minutes. Talwani's method, using a polygon with 35 sides to approximate the Goodrich quartzite required about 9 minutes.

ANOMALY RESOLVING TECHNIQUES

Five different methods were used to remove the regional anomaly. They are as follows:

- 1. Smooth contours.
- 2. Empirical grids.
- 2nd derivative methods.
- 4. Least squares polynomial analysis.
- 5. Downward continuation.

Smooth Contours

The smooth contour method, while not used extensively in this study, is a quick and simple way of estimating the regional anomaly. The method consists of drawing a smooth curve along the line of the estimated regional gradient as shown in Figure 10.

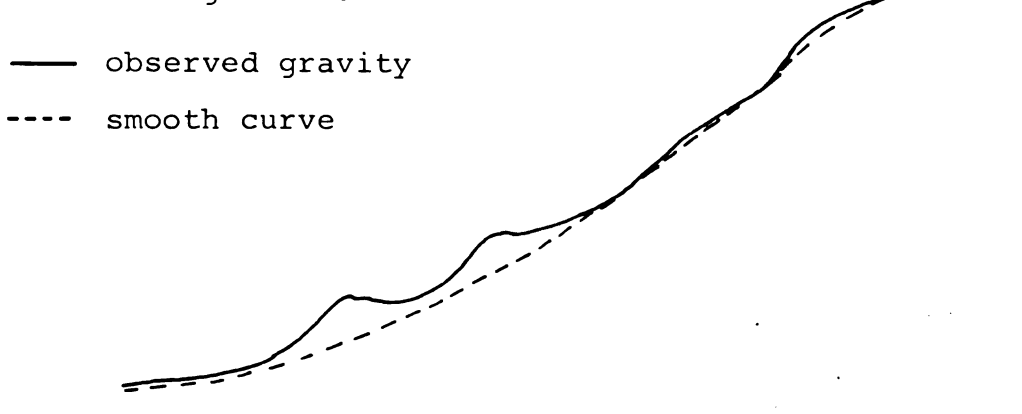


Figure 10

The smooth curve values are subtracted from the observed (or calculated) gravity curve and the residual anomaly remains.

The method has its shortcomings if the residual is of low magnitude or is superimposed on a steep gradient.

Empirical Grids

This method consists of using the mean of a number of values located on a ring, square or some geometrical figure as the regional, and subtracting this mean from the value of the point located at the center of the geometrical figure.

That figure which remains after subtraction is to be considered

the residual anomaly. Its value may be negative, zero, or positive.

The method used in this study consisted of a center point and four values located on a ring of radius r. A graphical picture of the method appears in Figure 11 as applied to a field of points.

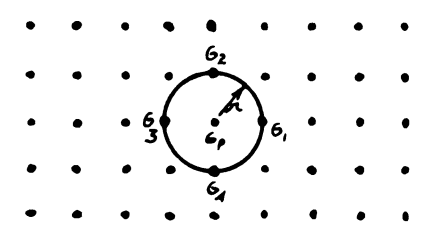


Figure 11

Griffen (1949) gives the following definitions for residual gravity expressions:

$$\Delta g = \text{residual gravity},$$
 $g_{o} = \text{gravity value at a point on a map, (profile)},$
 $\overline{g}(n) = \frac{1}{2\pi} \int_{0}^{2\pi} g(n, \Theta) d\Theta$, (25)

 $\vec{g}(n)$ is the average value at the radial distance r from the point where g_0 is observed; thus,

$$\Delta g = g_0 - \bar{g}(x) \quad . \tag{26}$$

Griffen further states that $\bar{g}(n)$ represents a form of g(n,e) which is not easily integrated. However, the function may be approximated by:

$$\bar{g}(n) = \frac{g_i(n) + g_{i+1}(n) \dots g_m(n)}{n} , \quad (27)$$

where $g_m(n)$ are the gravity values at a distance r from the point being evaluated, and

$$\Delta g = g_o - \bar{g}(\pi). \tag{28}$$

Griffen has found the size of the figure effects the residual value more than the shape of the figure.

Referring to Figure 11, the residual gravity at g. would be:

$$\Delta g = g_0 - \frac{g_1 + g_2 + g_3 + g_4}{4} \cdot (29)$$

A necessary requirement was to adapt the use of the empirical grids to two-dimensional form. This adaption was made by considering the gravity values constant in the y-direction as shown in Figure 12.

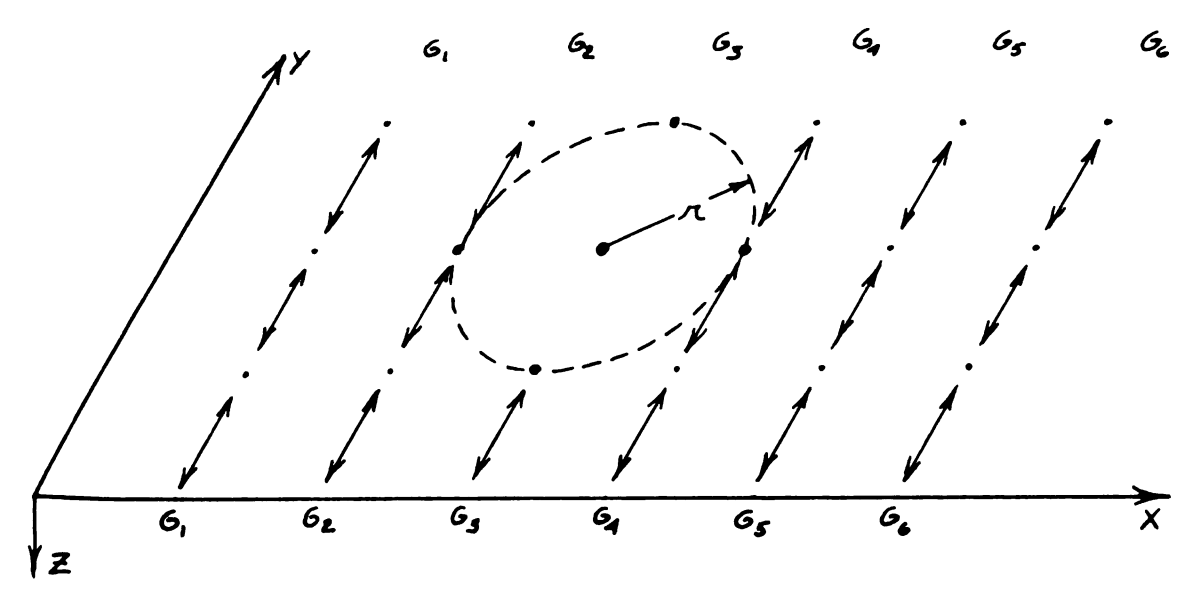


Figure 12

Therefore, if it were desired to determine the residual of, say, point G in Figure 12, the function would now be:

$$\Delta g = g_3 - \frac{g_2 + (2 \cdot g_3) + g_4}{4} , \qquad (30)$$

where:

$$\Delta g$$
 = residual gravity.

If the circle is replaced with a square;

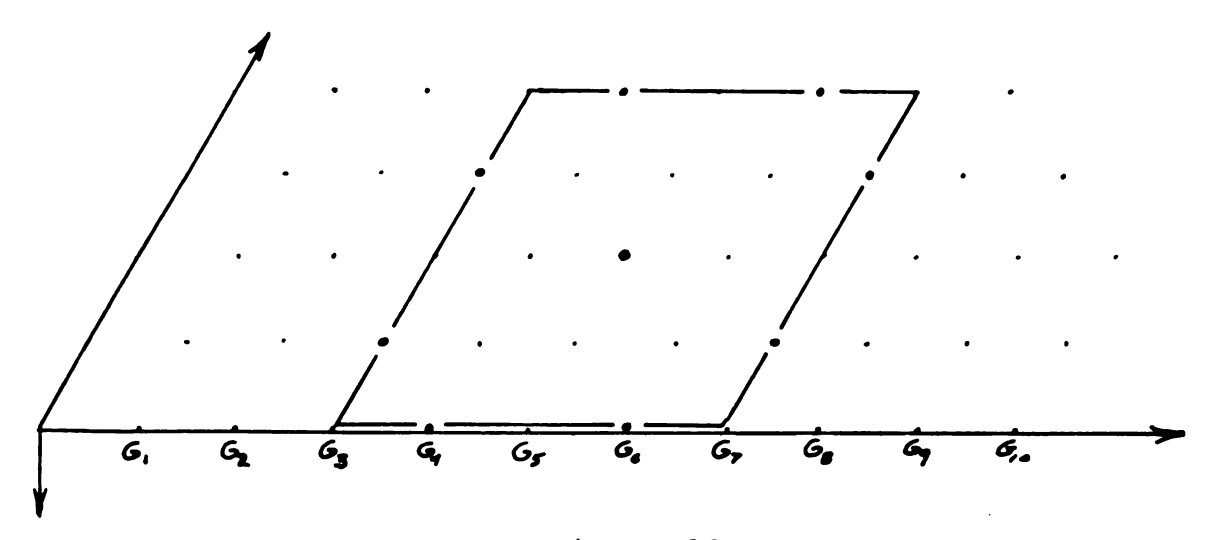


Figure 13

The equation becomes, as it is pictured in Figure 13,

$$\Delta g_5 = g_5 - \frac{(2 \cdot g_3) + (2 \cdot g_4) + (2 \cdot g_6) + (2 \cdot g_7)}{8} \quad (31)$$

Station spacing was maintained at 100 foot intervals.

2nd Derivative Methods

The 2nd derivative method of interpreting gravity data offers a simple routine method of locating some types of geological anomalies of importance in mineral exploration.

The method's importance arises from the fact that this type of analysis tends to emphasize the smaller, shallower geologic features at the expense of larger, regional features. It is for this reason that the 2nd derivative interpretation of a gravity anomaly often gives a clearer and better resolved picture of the type of anomaly than does the original gravity picture.

The analytical grid method of approximating the 2nd vertical derivative of gravity is similar to the empirical grid method. The empirical grids evolve from a simple statistical treatment, while the analytical grid methods are derived by a rather rigorous mathematical treatment of the theory of harmonic motion. The subject is well treated by Evjen (1936); Peters (1949); Henderson and Zietz (1949); Elkins (1951), and Rosenbach (1953).

Any function which has continuous 2nd derivatives at H(0,0,0) which satisfy Laplace's equation,

$$\frac{\partial^2 \mathcal{H}}{\partial X^2} + \frac{\partial^2 \mathcal{H}}{\partial Y^2} + \frac{\partial^2 \mathcal{H}}{\partial Z^2} = 0 , \qquad (32)$$

may be an harmonic function. Since the theory is being applied to gravitational attraction, which is assumed to be an harmonic function, the following substitution shall be made: $H(0,0,0) \equiv G(0,0,0)$

$$\frac{\partial^2 \mathcal{H}}{\partial X} = \frac{\partial^2 G}{\partial X^2} , \quad \frac{\partial^2 \mathcal{H}}{\partial X^2} = \frac{\partial^2 G}{\partial X} , \quad \frac{\partial^2 \mathcal{H}}{\partial Z^2} = \frac{\partial^2 G}{\partial Z^2}$$

It is desired to determine the 2nd vertical derivative $\begin{bmatrix} \mathbf{\partial}^2 \mathbf{G} \\ \mathbf{\partial} \mathbf{Z}^2 \end{bmatrix}$ $\mathbf{x} = \mathbf{y} = \mathbf{z} = 0$. By letting gravity represent the harmonic function on the plane $\mathbf{z} = 0$, and defining $\mathbf{G}(\mathbf{r}, \mathbf{z})$ to be

$$\bar{G}(\Lambda,Z) = \frac{1}{2\pi} \int_{0}^{2\pi} G(\Lambda,\cos\Theta,\pi\sin\Theta,Z) d\Theta , \qquad (33)$$

and $\overline{G}(r, z)$ at z = 0 is $\overline{G}(r)$, equation (33) becomes

$$G(\pi) = \frac{1}{2\pi} \int_{0}^{2\pi} G(\pi \cos \theta, \pi \sin \theta, \sigma) d\theta, \quad (34)$$

G(r), therefore, represents the average value of G(x, y, z) around a circle of radius r in the plane z = 0 with the origin as the center of the circle. By its relationship to G(x, y, z), G(r) may be expanded in a power series in r about r = 0 so that

$$\bar{G}(\pi) = a_0 + a_2 \pi^2 + a_4 \pi^4 + a_6 \pi^6 \dots$$
 (34a)

where the odd powers of r are absent because integration of equation (34) contains $\sin \theta$ and $\cos \theta$. Since these two terms reach odd powers and have a period of $2\,\%$, they become zero.

It is through the use of G(r) that the 2nd derivative of G(x, y, z) may be obtained. By transposing equation (32) we obtain

$$\frac{\partial^2 G}{\partial Z^2} = -\left(\frac{\partial^2 G}{\partial X^2} + \frac{\partial^2 G}{\partial Y^2}\right) \qquad , \tag{35}$$

and by letting $x = \pi \cos \theta$, $y = \sin \theta$, equation (35) becomes

$$\frac{\partial^2 G}{\partial z^2} = -\left(\frac{\partial^2}{\partial n^2} - \frac{1}{n}\frac{\partial}{\partial n} + \frac{1}{n^2}\frac{\partial^2}{\partial \theta^2}\right)G , \qquad (36)$$

If equation (36) is integrated with respect to 0 between the limits of 0 and 2 \mathcal{T} , and for $\mathcal{T} > 0$ and at z = 0 we are able to obtain

$$\frac{\partial^2 G}{\partial Z^2} = \frac{1}{277} \int_0^{277} \frac{\partial^2 G \left(\mathcal{R} \left(OS\Theta, \mathcal{R} S / N\Theta, Z \right) \right)}{\partial Z^2} d\Theta , \quad (37)$$

$$\frac{\partial^2 G}{\partial Z^2} = -\left(\frac{\partial^2}{\partial n^2} + \frac{1}{n} \frac{\partial}{\partial n}\right) \bar{G}(n) , \qquad (37a)$$

Now by letting π approach 0 and making use of the power series describing $\overline{G}(r)$, (equation 34a), the following formula is obtained:

If some point is picked in the plane z=0 as a center and a plot is made of the average value of G in a plane around a circle of radius π versus π^2 , the slope of the plotted curve is the derivative of \bar{G} with respect to π^2 .

The process of finding the value of a in equation (38) requires the following assumptions:

- 1. Choose an π small enough so G(r) has enough terms (equation 34a) to represent it accurately.
- 2. The curve G(r) is replaced by a straight line.
- 3. The mean value of $\overline{G}(r)$ for circles of radii of S(0), S, SVZ, SVS about a point gives four distinct points on a graph of $\overline{G}(r)$ versus Λ^2 .

These points are:

$$\vec{G}(0)$$
, $\vec{G}(5)$, $\vec{G}(5VZ)$ AND $\vec{G}(5V\overline{5})$. (39)

Since these four points lie on a curve which may not go through the origin, a linear least squares fit is made and the slope of this line replaces $\frac{\partial G}{\partial (\Lambda^2)}_{\Lambda} = 0$

As a result of this approximation, equation (38) is replaced by:

$$\frac{\partial^2 G}{\partial Z^2} = -4\alpha_2 = \frac{1}{625^2} \left[44 \, \bar{G}(0) + 16 \, \bar{G}(5) - 12 \, \bar{G}(5 \, VE) - 48 \, \bar{G}(5 \, VS) \right] . \quad (40)$$

The above derivation has been adapted from Elkins (1951). Figure 14 shows Elkins' grid method applied to a field of points.

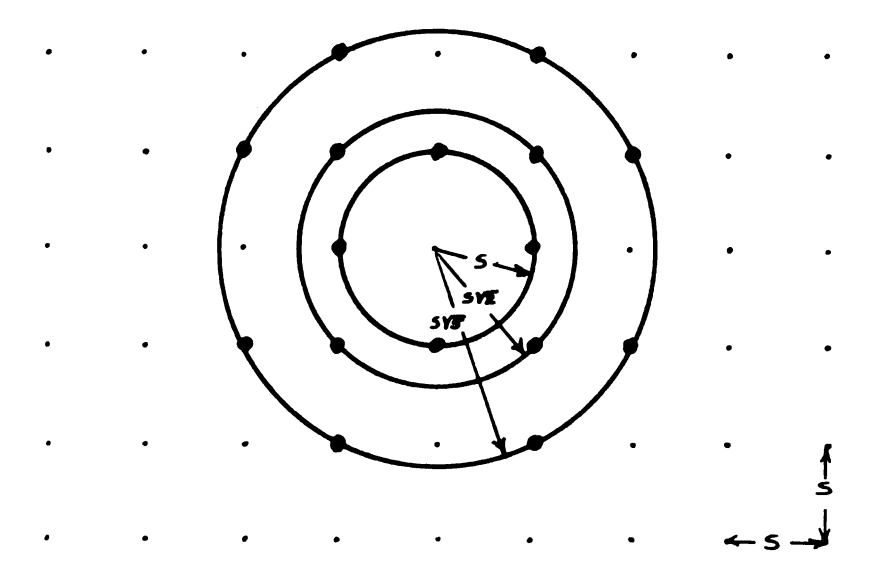


Figure 14

The following formulas were used in this study where

$$GZZ = \frac{3^2G}{5Z^2} , \qquad (41)$$

Baranov

$$GZZ = \frac{0.1}{5!} \left[5.76g_{p} - 1.85 \sum_{i=1}^{4} g_{i}(5) + 0.4 \sum_{i=1}^{4} g_{i}(5) + 0.005 \sum_{i=1}^{8} g_{i}(5) + 0.005 \sum_{i=1}^$$

Henderson and Zietz

$$GZZ = \frac{1}{25^2} \left[12g_{\rho} - 4\sum_{k=1}^{4} g_{k}(S) - \sum_{k=1}^{4} g_{k}(SVZ) \right] , \qquad (43)$$

Elkins (I)

$$GZZ = \frac{1}{625} \left[4g_{p} + 4\sum_{i=1}^{4} g_{i}(S) - 3\sum_{i=1}^{4} g_{i}(SVZ) - 6\sum_{i=1}^{8} g_{i}(SVZ) \right], \quad (44)$$

Elkins (II)

$$GZZ = \frac{1}{665!} \left[204g_{p} - 12 \sum_{k=1}^{4} g_{k}(S) - 47 \sum_{k=1}^{4} g_{k}(SVZ) + 4 \sum_{k=1}^{8} g_{k}(SVS) \right], (45)$$

Rosenbach (I)

$$6ZZ = \frac{1}{245^{2}} \left[96g_{p} - 18 \sum_{i=1}^{4} g_{i}(S) - 8 \sum_{i=1}^{4} g_{i}(SVZ) + \sum_{i=1}^{4} g_{i}(SV\overline{S}) \right], \quad (46)$$

McCollum (altered)

$$6ZZ = \frac{1}{125^2} \left[60g_{\rho} - 16\sum_{i=1}^{4}g_{i}(5) + \sum_{i=1}^{4}g_{i}(5\sqrt{2}) \right], \qquad (47)$$
*McCollum gives last term as $g_{i}(25)$.

Haalck

$$6ZZ = \frac{1}{4S^2} \left[12g_{*} - 2\sum_{i=1}^{4} g_{i}(S) - \sum_{i=1}^{4} g_{i}(SVZ) \right] , \qquad (48)$$

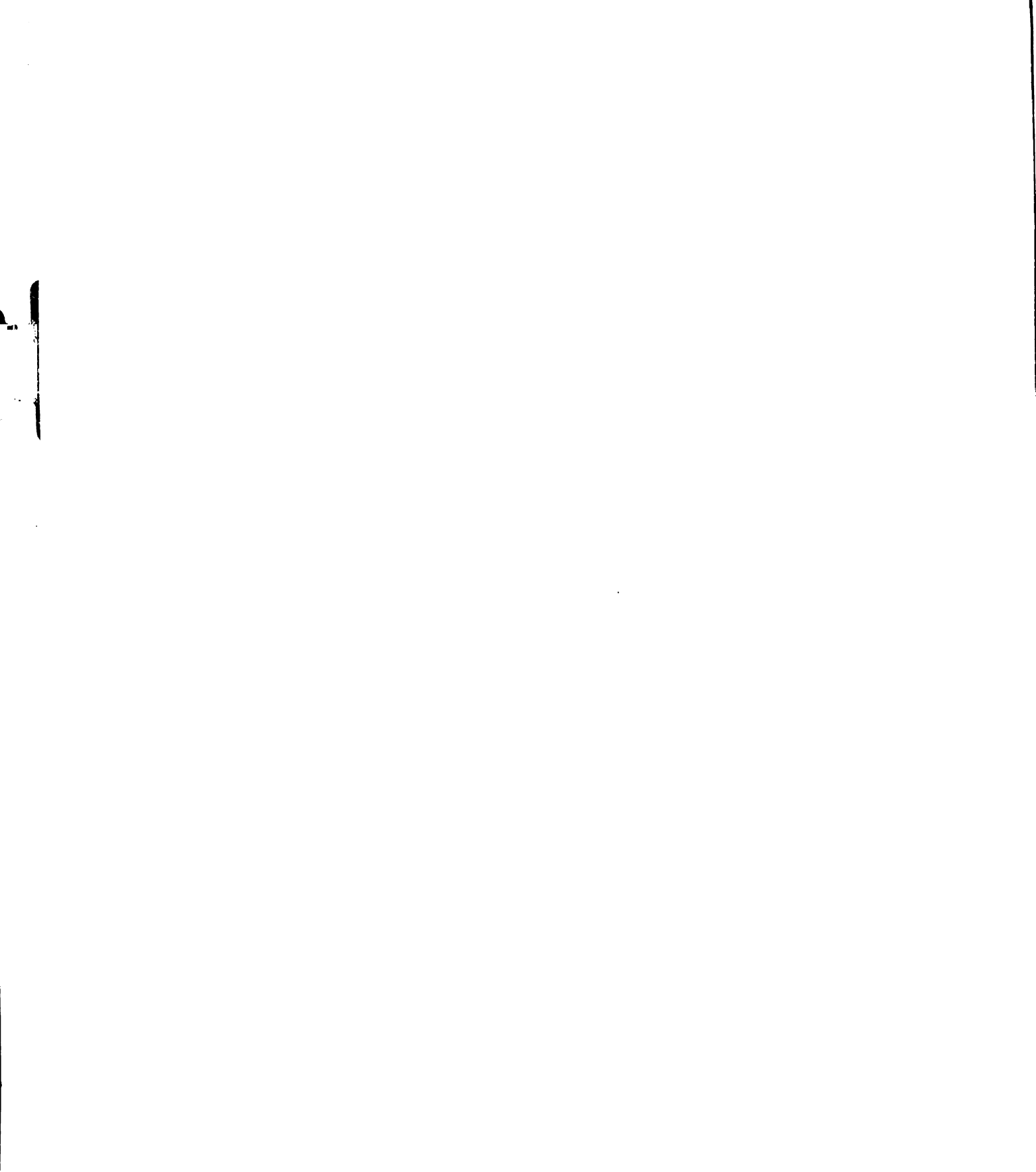
It is interesting to note that the sum of all the weighting coefficients must equal zero. In addition, all the formulas involve a term of $\frac{1}{4.5^2}$ where s is the radius of the inner circle. Nettleton (1954) attempts to explain the $\frac{1}{5^2}$ term as similar to an electric filter in which the s or station spacing factor controls the components of the potential field which the analytical grids were devised to analyze. The ideal grid being that system which amplifies or emphasizes those anomalies which indicate structure and attenuates or suppresses those components which are superficial or those too broad to be of interest.

All of the above analytical grid methods were converted into computer programs and each method used on the theoretical geologic cross-sections and the case histories. The results of this analysis will be discussed later.

As in the case of the empirical grids, this method was also reduced to a two-dimensional form for use in this study. Station spacing was maintained at 200 foot intervals.

Least Squares Polynomial Approximation

The method of least squares has long been used to obtain a linear best fit of a discreet set of data points. It has been only recently that the method of least squares has been



applied to gravity data using high degree polynomials.

In simple terms, the reason for its use in gravity data analysis is to generate a polynomial which may be used to approximate the regional anomaly in a gravity profile.

Let the profile of gravity values as shown in Figure 15

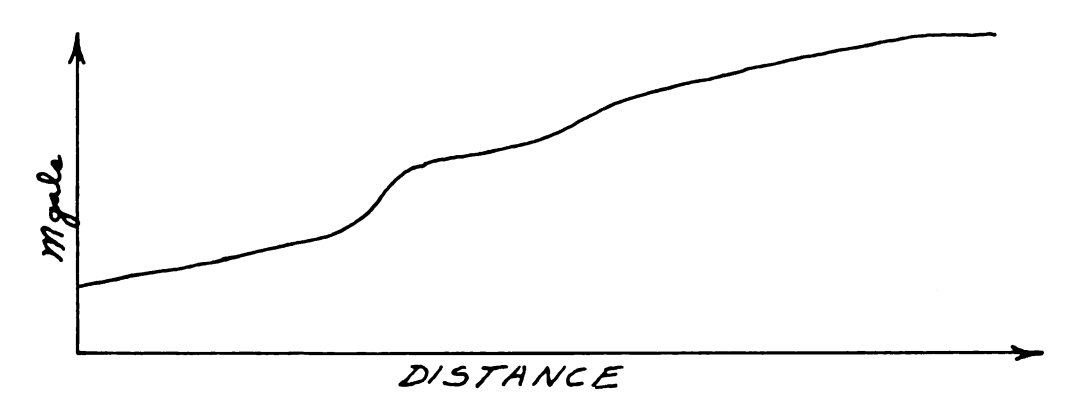


Figure 15

represent functional values of x, that is, y = f(x); also let the station spacing become the independent variable x. As shown in Figure 16, a gravity profile may then be represented as some function of x and y.



Figure 16

It would be convenient in the analysis of gravity data if the curve, f(X), could be approximated by a polynomial of some degree which closely, but not exactly, matched the original f(X) values.

This is precisely what the least squares method as applied to gravity data can do. In brief form, the theory behind the method states that the aggregate sum of the squared errors be a minimum or

$$R(X)^2 = \left[f(X) - P_{\nu}(X) \right] = \text{a minimum} \tag{49}$$

where:

R(X) = error between f(x) and the least squares polynomial,

 $P_{\mu}(X)$ = least squares polynomial,

f(x) = functional values of x (gravity).

By letting the least squares polynomial of various degrees represent the regional gravity anomaly, that part of the gravity curve which is in greatest error with the least squares polynomial becomes the residual anomaly.

This method was applied to the four computed gravity profiles and the two observed gravity profiles. Polynomials whose degree ranged from 1 to 10 were obtained and used to approximate the profiles. It was not possible to obtain higher order fits

because of the limited size and storage capacity of the Control Data 160A computer. However, the 10th degree fit was, in most cases, sufficient to approximate the regional.

The general procedure was to obtain all degrees, from 1 to 10, and then determine which degree met the requirements of the gravity profile.

There are some areas of least squares polynomials derived by a digital computer which cause some difficulty, particularly if the computer being used is small in terms of core memory and word length. The method of least squares consists primarily of a series of tabulations and the construction and solution of a matrix consisting of the coefficients of a number of linear equations. While the problem is clear cut and easily programmed, it must be remembered that within the matrix of coefficients there are numbers whose values increase up to as high as 1.0 x 10^{20} for a low degree equation. Since the number range on the Control Data 160A is within the bounds of 1.0 x 10^{-30} to 1.0 x 10^{31} , it is possible to introduce serious errors by exceeding this limit. There are several methods of suppressing the problem so that a polynomial of higher degree may be obtained. One simple and effective method is to reduce the range of x values used within the program.

Thus, if the input data consists of x values, from 1.0 to 90.0 numbered consecutively, it is possible to reduce their range to 0.1 to 9.0. This permits the computer to operate on the various powers of x with greater efficiency and with less roundoff error. For example, $90^5 = 5.9 \times 10^9$ while $9.0^5 = 5.3 \times 10^5$. While this is a simple case, it does illustrate how to make more effective use of the computer.

The following list will serve to indicate the usefulness of the method. The list consists of the error $R(x)^2$ for a set of data. The set of values range from 0.1 to 9.0. The smaller $R(x)^2$ value indicates the better approximations by the polynomial to the gravity data.

Penokee-Gogebic

Table 1

Degree Polynomial	R(x) Value
1	11 704
1	11.784
2	10.068
3	3.537
4	2.634
5	1.553
6	1.103
7	1.174
8	1.093
9	1.113
10	0.945
*18	0.261

^{*}computed on the Control Data 3600 computer.

It should also be stated that the $R(x)^2$ value will not necessarily decrease in magnitude with increasing power of the approximating polynomial. This is due to the fact that in the least squares method, all the values of f(x) are used, that is, during the tabulation of the x and f(x) values the entire range of these values are taken into account. This results in polynomials which may on a certain degree approximate different parts of the original data curve better than another degree polynomial. For example, a 6th degree fit may give a good approximation of the end points of the curve and yield an $R(x)^2$ term which is lower than a 7th degree fit which shows better approximation in the central part of the curve and poor correspondence at the end thereby yielding a high $R(x)^2$ term.

Downward Continuation Methods

The theory behind the method of continuing a potential field downward toward its source can be credited to Bullard and Cooper (1948); Peters (1949), and Trejo (1954).

While the resolving power of the downward continuation method is not as great as the derivative methods of isolating anomalies, it does have the advantage of retaining the results

in familiar units. In brief, the method greatly increases the amplitude of near surface anomalies and increases only slightly the amplitude of the anomaly over deep-seated or regional features.

The two methods used in this study were the fivepoint and nine-point downward continuation for the twodimensional case. The two methods were developed by the
Department of Geology, geophysics section, Michigan State
University. The two methods are derived by the theory of
finite differences and the relaxation methods as used by
Bullard and Cooper.

The formulas for the two methods are:

a) Five-point downward continuation:

$$D_5 = 3.6817(H) - 1.15915(A+C) - 0.1817(E+F)$$
,

b) Nine-point downward continuation:

$$D_q = 3.6817(H) - 1.15915(A+c) - 0.06366(E+F)$$

-0.3183(I+J) - 0.08621(K+L).

R is the distance the field is continued downward, where A,

C, E, F, I, J, K, L, and H are gravity values located a distance

R from each other. Station spacing was at 100 foot intervals

and the field was continued down 100 feet.

INTERPRETATION OF RESULTS

The interpretation of gravity anomalies has as its objectives the determination of density, shape, and depth of subsurface bodies. According to Skeels (1947), this is an impossible task since there are an infinite number of mass arrangements which may produce the same gravity anomaly. However, in practice, the task becomes surmountable since other factors such as application of other geophysical methods and the geological possibilities of the area may be considered.

One established procedure in making a tentative interpretation is to consult a family of theoretical gravity curves for common geologic features. By consulting these curves and considering the geologic possibilities, some picture of the subsurface conditions may be obtained.

A more quantitative interpretation may be used to supplement the qualitative procedures. Definite densities, shape, attitude, and depths are assumed and their gravity effects are calculated. These results are then compared with data which has been gathered in the field. This trial and error method is used until some satisfactory agreement is reached.

In utilizing the formulas and methods which permit a quantitative approach, the restriction of long, tedious computations must be considered. With the use of the digital computer this restriction is removed and the method becomes flexible and adaptable to many types of problems. The depth, density, shape, and attitude may be altered at will and results available within a matter of minutes, which formerly would have required days to obtain.

Shown on Plates I, II, III, and IV are the four gravity profiles calculated with the above mentioned quantitative methods. Also shown on the plates are the geologic crosssections over which the gravity was computed. In addition, the various 2nd derivative interpretations and an empirical grid interpretation of the profile are drawn below the section. In order to show the correlation of the 2nd derivative interpretations with the gravity profile, the interpretive curves are listed below the geologic cross-section.

The methods of smooth curves, downward continuation, and least squares are shown in individual figures.

Amasa Oval

General Discussion. On Plate I the geologic crosssection is shown with the individual gravity profile for each formation drawn above it. Directly above this series of curves and appearing at the very top of the plate is the total gravity profile across the section.

It is apparent that the two major influences of this cross-section are the Hemlock formation and the Michigamme slate. The effects of the Margeson Creek gneiss and Rand-ville dolomite are of minor influence, causing only a slight increase on the west end of the profile. Superimposed on the total gravity curve is the residual anomaly caused by the Fence River formation. The entire cross-section was computed with a depth to the top of the formations of 100 feet. The total depth of the section is 3,000 feet. The length of the profile is 9,300 feet with gravity values computed at 100 foot intervals. All of the curves of Plate I were plotted on the digital computer plotter and then traced on to Plate I.

Interpretation of 2nd Derivative and Empirical Grid
Results. Shown on Profile A, Plate I, are the analytical
grid methods for determination of the 2nd derivative values.
On Profile A the methods of Henderson and Zietz, Rosenbach,
Haalck, Elkins II, and McCollum are drawn on the same axis
to show the very close correspondence each of these methods
has with the other. There is only slight variation in the

amplitudes of each of the methods and all the curves cut the zero axis of the profile at the same point.

On Profile A there are three anomalies shown. first anomaly at the west end, while not discernible on the gravity profile across the section, is created by the contact between the Margeson Creek gneiss and the Randville dolomite. It is the first positive to negative change at the west end of Profile A. It should be noted that this slight anomaly is caused by the original computations used to derive the total gravity profile. These computations were carried out to an accuracy of 0.00001 mgal. As the individual gravity curves were added up to produce the total curve, there is noticeable increase and decrease in the gravity values as the summation proceeds across this contact between the Margeson Creek gneiss and the Randville This increase and decrease of values occurs at the 3rd and 4th decimal place and is not visible when the values are plotted on the scale used in plotting the gravity profile.

The second anomaly occurs at the contact between the Randville dolomite and the Hemlock formation. The 2nd derivative curve crosses the zero line at exactly the same location as the surface contact of the two formations.

The third anomaly, that due to the anomaly over the Fence River formation, is outstanding in appearance. The peak of the anomaly centers on the middle of the Fence River formation. The curve approaches its near maximum negative value and then changes direction, reaches its peak and reverses itself and plunges to its maximum negative value again, finally becoming asymtotic to the zero line. The width of the anomaly at the zero line is about 400 feet as compared with the width of 200 feet of the Fence River formation at the surface.

When observing Profile B, which shows the Elkins I method, the first appearance is that there is a marked similarity between this curve and that of the total gravity curve. In addition, there are no negative values on the profile. These two features are caused by Elkins' choice of coefficients within his analytical grid formula.

The curve clearly outlines the major anomalous areas of the profile. Some assumption could possibly be made about the attitude of the Fence River formation based on the asymmetrical shape of the anomaly over that formation.

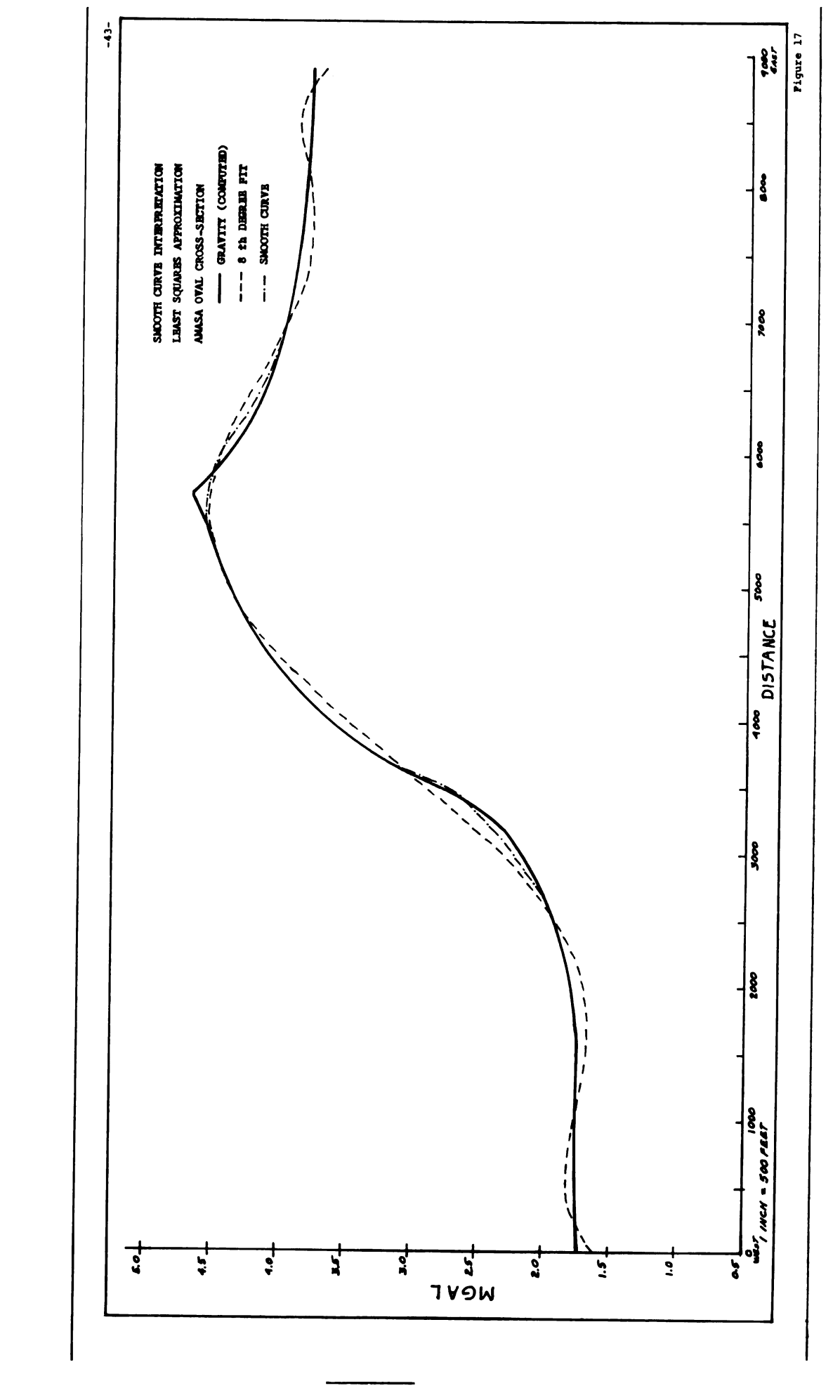
Profile C shows the results of the empirical grid method and appears as a damped version of Profile A. For this type

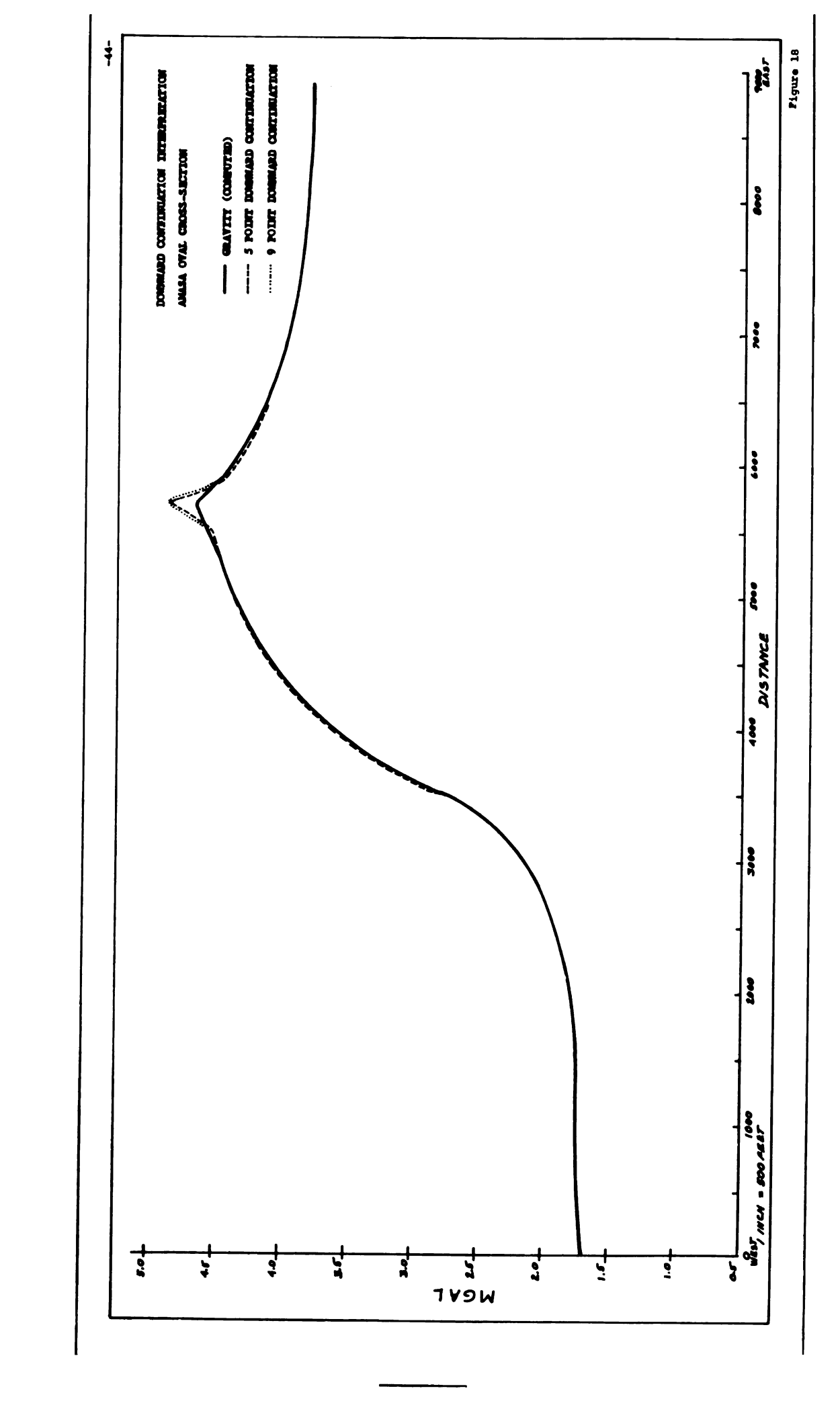
of study it appears that this rather simple method is as useful as the more complex analytical grids, and requires fewer computations.

An additional advantage is that the resulting residual values are expressed in milligals and not the rather cumbersome 1.0×10^{-9} (mgal/cm²).

Smooth Curve and Least Squares Interpretation. On Figure 17 is shown the 8th degree approximation to the original gravity profile of the Amasa oval cross-section. The 8th degree fit was selected because it gave a better overall fit to the data than did the other orders. While the approximating curve does not isolate the residual anomaly as do the 2nd derivative methods, it does, however, eliminate much of the large anomaly caused by the Hemlock formation. The smooth curve, also drawn on this sheet includes much of the Hemlock formation anomaly, which would result in a residual anomaly of entirely different magnitude. This may be purely speculative since the matter of personal choice and bias enter into the picture.

Downward Continuation Interpretation. The five-point and nine-point downward continuation methods shown on Figure 18 both yielded an exceptionally fine isolation of the anomaly





caused by the Fence River formation. The amplitude of the two resultant curves differs by only 0.3 mgal. The method leaves little doubt as to the location of the residual anomaly.

Michigamme Mountain

General Discussion. The cross-section of the Michigamme Mountain area is shown on Plate II with the resulting gravity profiles of the formations present. The total gravity curve for the cross-section is the upper curve of the plate. Shown also are the various 2nd derivative interpretations of the gravity profile.

In this cross-section the Goodrich quartzite appears as a wedge-shaped formation which pinches out downdip. This cross-section, in the strictest sense, does not meet all of the requirements set forth on page 3. However, some criteria had to be used to test the validity of the methods used in calculating the gravity profiles. By comparing Heiland's and Talwani's method on this type of structure, some judgment could be made concerning the overall performance of both methods. Heiland's method yields results comparable to Talwani's in accuracy. Heiland's method works well and with moderate speed for simple structures when programmed on the Control Data 160A computer.

Talwani's N-sided polygon method is exceptionally fast for simple and complex structures and gives results which have a close correspondence to Heiland's.

A comparison of the results shows that both methods gave the same results, with Talwani's method used on a 35-sided polygon, and Heiland's method using 30 foot tabular-shaped approximations.

Interpretation of 2nd Derivative and Empirical Grid
Results. All of the methods used to interpret the rather
simple anomaly shown on the plate, with the exception of
Elkins' I method, clearly isolate the anomaly. Elkins' I
is, in reality, a repetition of the original gravity curve,
with only the width of the original residual anomaly slightly
reduced.

There is some variation in the amplitude of the positive and negative anomalies of Profile A between the various methods. This is due to the choice of coefficients used in each method.

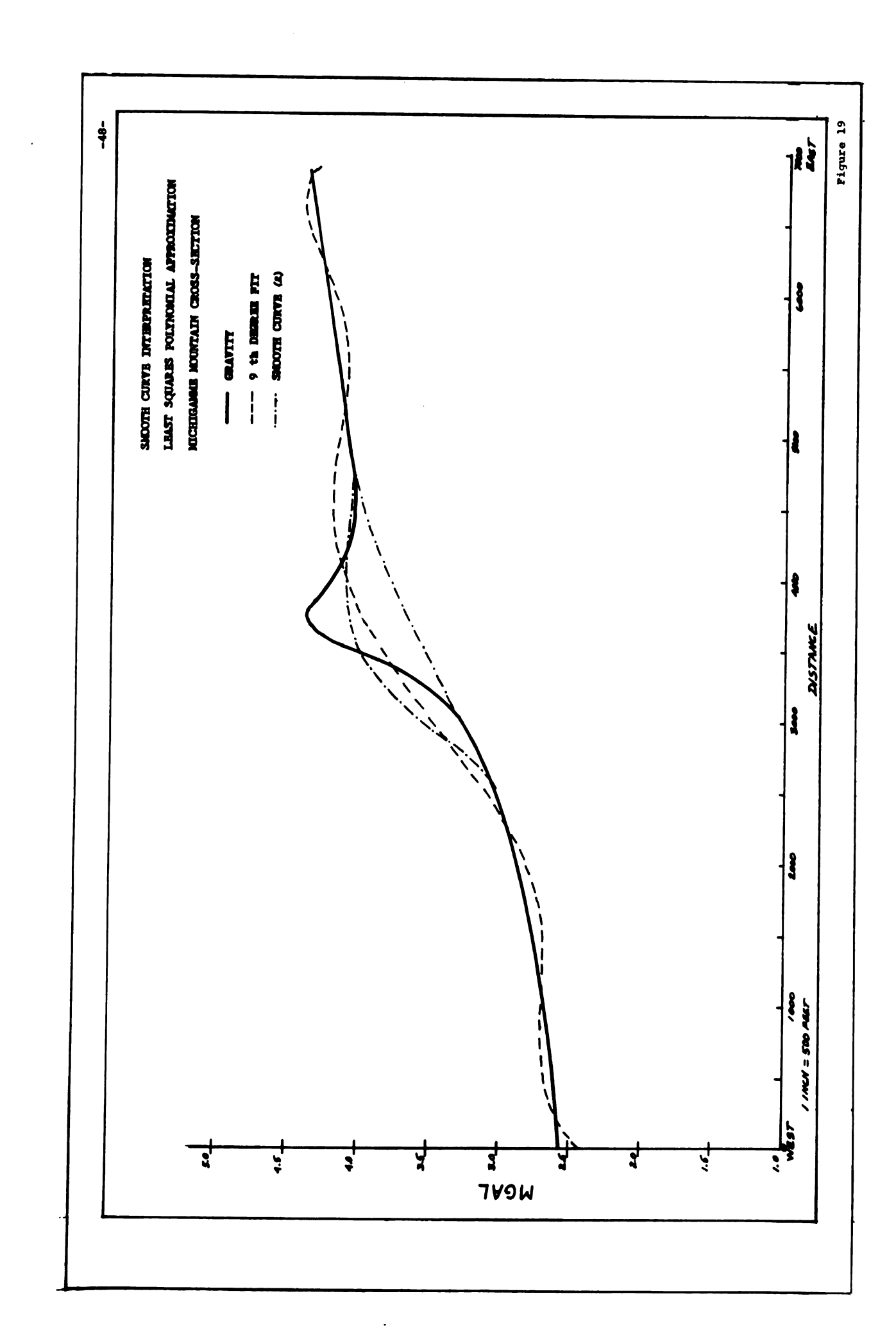
On Profile A and C the curves cross the zero line (from - to + and from + to -) giving a width equal to the original surface width of the Goodrich quartzite, which is 690 feet.

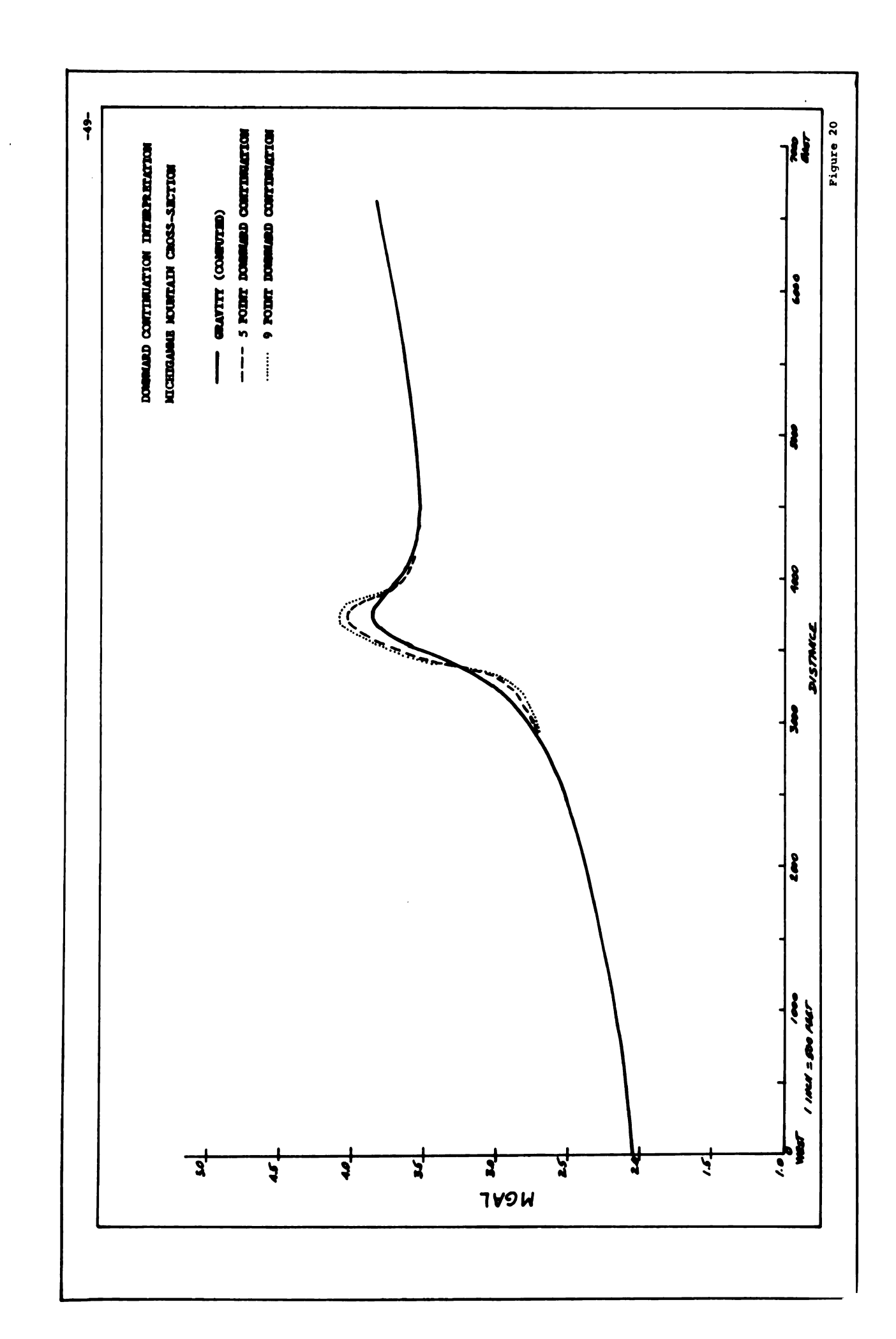
Smooth Curve and Least Squares Approximation. The curves on Figure 19 show the 9th degree approximation to the original gravity profile and the smooth curve estimate of the regional anomaly. Both curves are about the same in magnitude with the smooth curve giving a residual of larger amplitude than the 9th degree least squares curve.

The 9th degree fitting curve in this case crosses the original gravity curve at x = 3385 and x = 4075. This results in a residual anomaly having a width at the base of 690 feet, exactly that surface width of the Goodrich quartzite. It should be pointed out that this is an exceptional case, and is certainly not to be expected of the least squares method. In this particular example, with the gravity profile being simple in outline, the 9th degree curve crossed the original curve at these two points more by chance than any inherent design of the interpretive method.

Downward Continuation Interpretation. Figure 20 shows the curves for the five-point and nine-point downward continuation methods as applied to the original gravity profile.

The methods both accentuate the isolated Goodrich quartzite anomaly exceptionally well. There is about 0.06 mgal difference in magnitude between the two methods at the peak of the anomaly.





The width of the anomaly is reduced somewhat by both methods, which results in a sharp, isolated outline of the anomaly.

Marquette District

General Discussion. The cross-section of the Marquette area is shown on Plate III. This particular profile was selected because of the different variety of formations that were available for a quantitative analysis.

The lateral extent of 200,000 feet at each end of the profile does much to influence the outline of the gravity profile. However, this is strongly modified by the repetition of Kitchi schist and the peridotite masses at the north end of the section.

On Plate III only the gravity profile of the Negaunee iron formation is plotted along with the total gravity over the section. It can be seen that there is considerable regional anomaly by observing the separation between the peak of the Negaunee iron formation anomaly and the peak over the same area on the total gravity curve.

Interpretation of 2nd Derivative and Empirical Grid Methods.

Shown also on Plate III are two interpretations of the anomaly.

Profile A, using Rosenbach's method again clearly outlines the

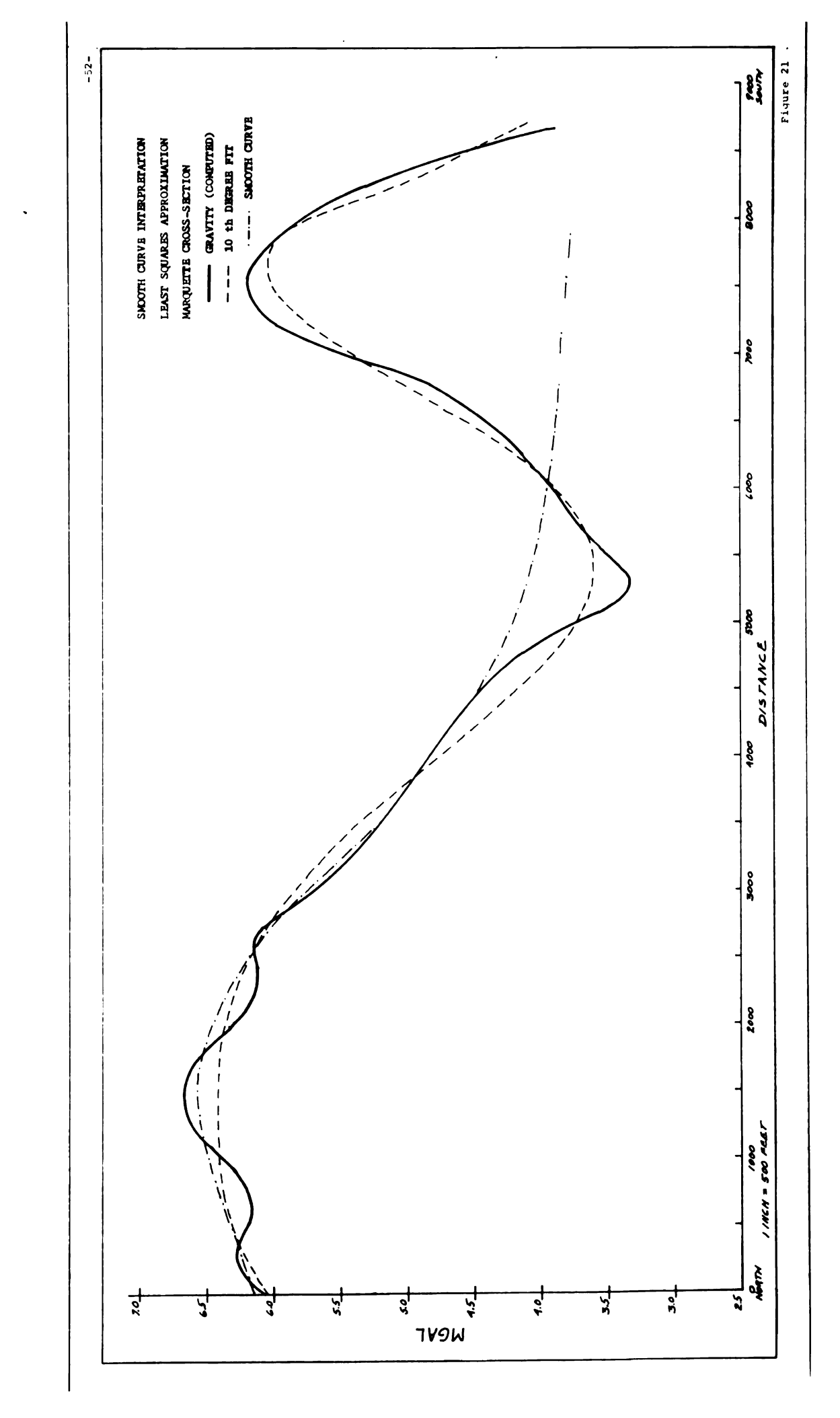
anomalous areas. In Profile B, using Elkins' I method, a better resolved picture of the original gravity curve appears.

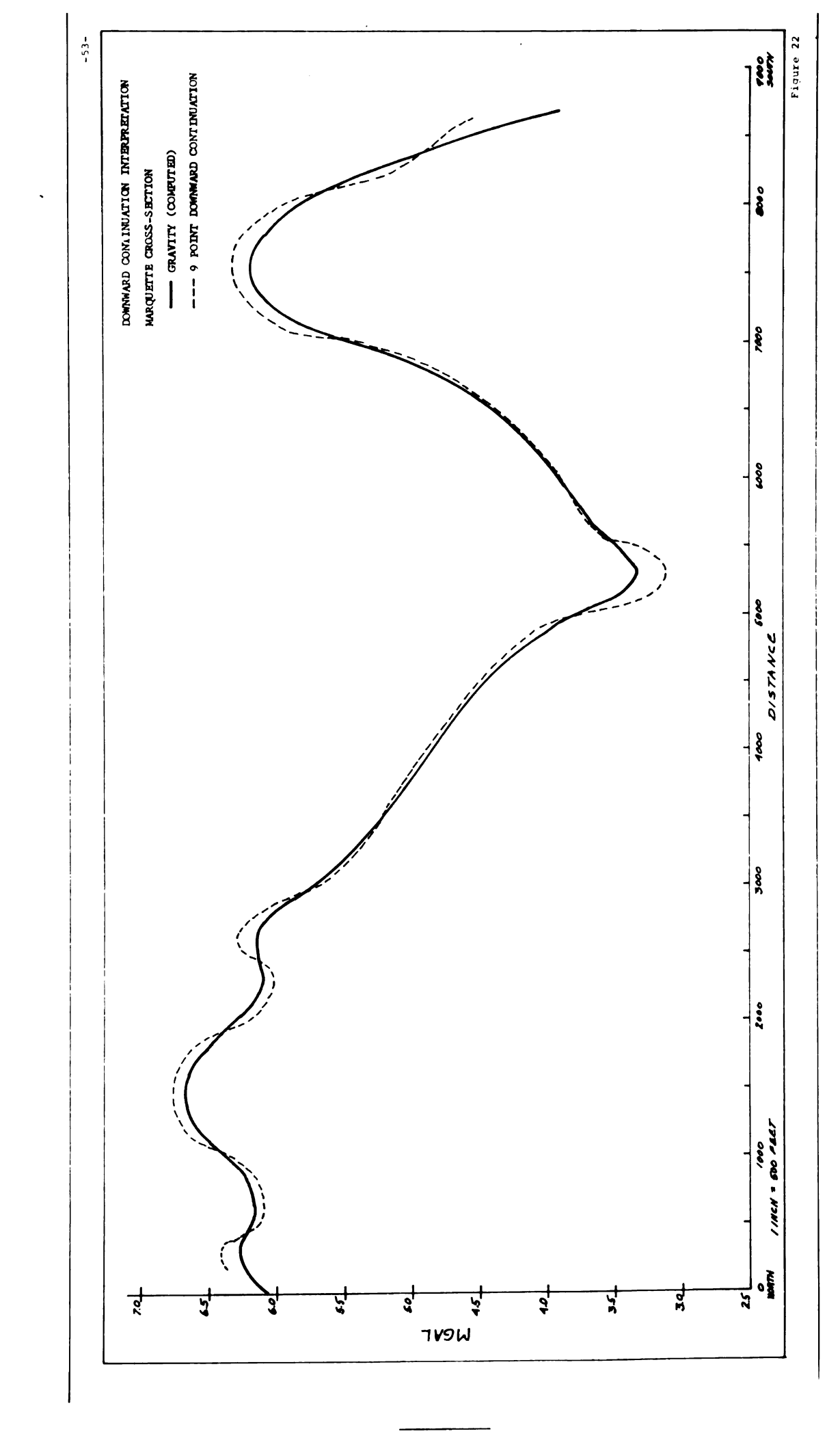
In Profile A the 2nd derivative curve crosses the zero line at points roughly equal in width to the width of the disturbing formation. In addition, the individual fluctuations are more symmetrical in outline. This would seem natural since the individual anomalies for each formation will give a symmetrical gravity curve, and these curves, when added together, will result in a profile roughly symmetrical in outline.

The empirical grid method, the average of four points on a circle, subtracted from the center point, was not utilized on this case due to the fact that the profile it produced was the same in appearance as those determined by the analytical grids.

Smooth Curve and Least Squares Approximation. The curves in Figure 21 represent the smooth curve estimate and the least squares approximation of the regional anomaly of the Marquette gravity profile.

It can be seen that the smooth curve estimate is a fairly valid one, since it isolates the anomalous regions with about the same accuracy as the 10th degree fit by least squares.





The smooth curve, however, does include much that is not considered regional by the 10th degree polynomial.

However, the smooth curve does give a better estimate of the magnitude of the Negaunee iron formation anomaly.

Downward Continuation Interpretation. The nine-point downward continuation method both accentuates and isolates both the positive and negative anomalies of the profile.

The nine-point method is shown on Figure 22. The isolation of the anomalous masses at the north and south end of the profile is well seen and the negative anomaly in the center of the section is well established.

Penokee-Gogebic

General Discussion. Plate IV illustrates the Penokee-Gogebic cross-section and the gravity profiles associated with it.

The individual gravity profiles in this section present an interesting picture of how the component parts of a total gravity profile combine to give a picture of residual anomalies superimposed on a steep regional gradient.

The two component profiles associated with the formations, having a density of 2.87 and 2.90, create the first residual

and the component profile of the formation with a density of 3.10 yields the second residual.

The major influence of the cross-section is the anomaly caused by the contact between the Tyler slate and the granite and granite gneiss.

The fact that the Ironwood formation is dipping in the same direction as the Tyler slate also helps mask the residual anomaly. This is well illustrated by observing the different profiles shown on Figure 28 and Figure 29 (pages 63 and 64). Figure 28 shows the Penokee-Gogebic gravity profile computed with all formations dipping 60° to the northwest. Figure 29 shows the same sequence of formations with all formations now vertical. The residuals now are well defined and not too difficult to isolate.

Figures 28 and 29 (page 63 and 64) point out two interesting facts. In Figure 28 which is the gravity for the cross-section dipping 60°, the magnitude of the gravity curve probably gives less information than does the slope of the curve. Dipping formations yield gravity profiles which are asymmetrical in appearance, with one side having a much steeper gradient than the other. In Figure 29, which is the gravity for the cross-section now assumed to be vertical in attitude, the magnitude

of the gravity profile gives a better clue to making an interpretation of the cross-section. This is because the gravity over a vertical formation gives a symmetrical outline with maximum amplitude whereas the same formation, if dipping, will give reduced amplitude but a maximum gradient on one side of the curve. It is apparent that attitude plays an important role in how a residual may become distorted by attitude as well as by regional gradient.

2nd Derivative and Empirical Grid Interpretations. The three different methods shown on Profiles A, B, and C of Plate IV all define and isolate the two anomalous areas of the gravity profile. They also indicate which of the two anomalies is the greatest in magnitude. Little information can be gained about the attitude of the formations from the 2nd derivative curves.

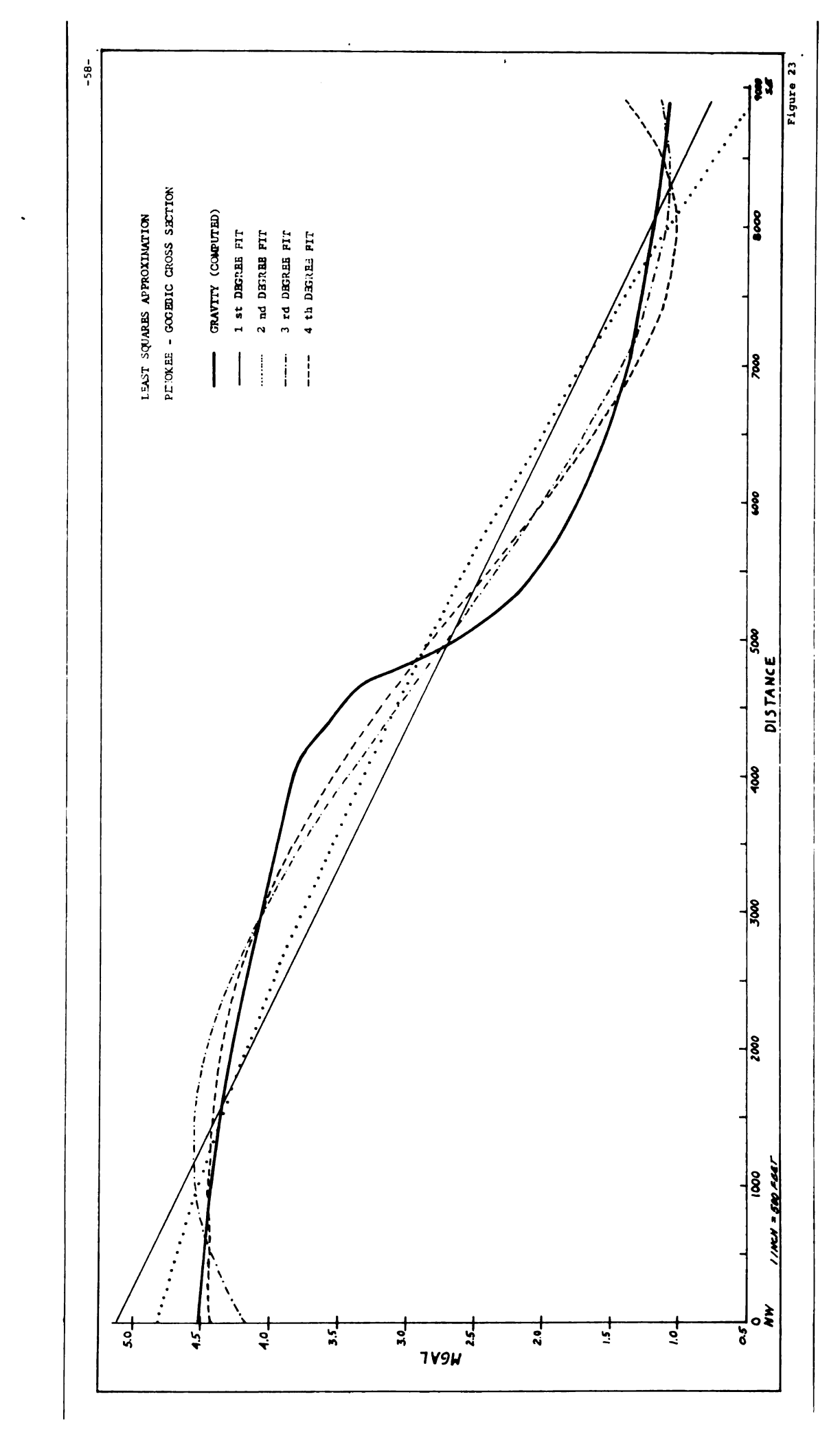
The presence of the Palms quartz slate, the unit next to the iron formation, might be assumed by the change of the 2nd derivative curves' slope as it rises from its maximum negative point and begins its asymtotic approach to the zero line, as shown in Profile A and B. This is also barely visible on Profile C, showing Elkins' I method. Formation widths determined from the 2nd derivative curve as it crosses the zero line

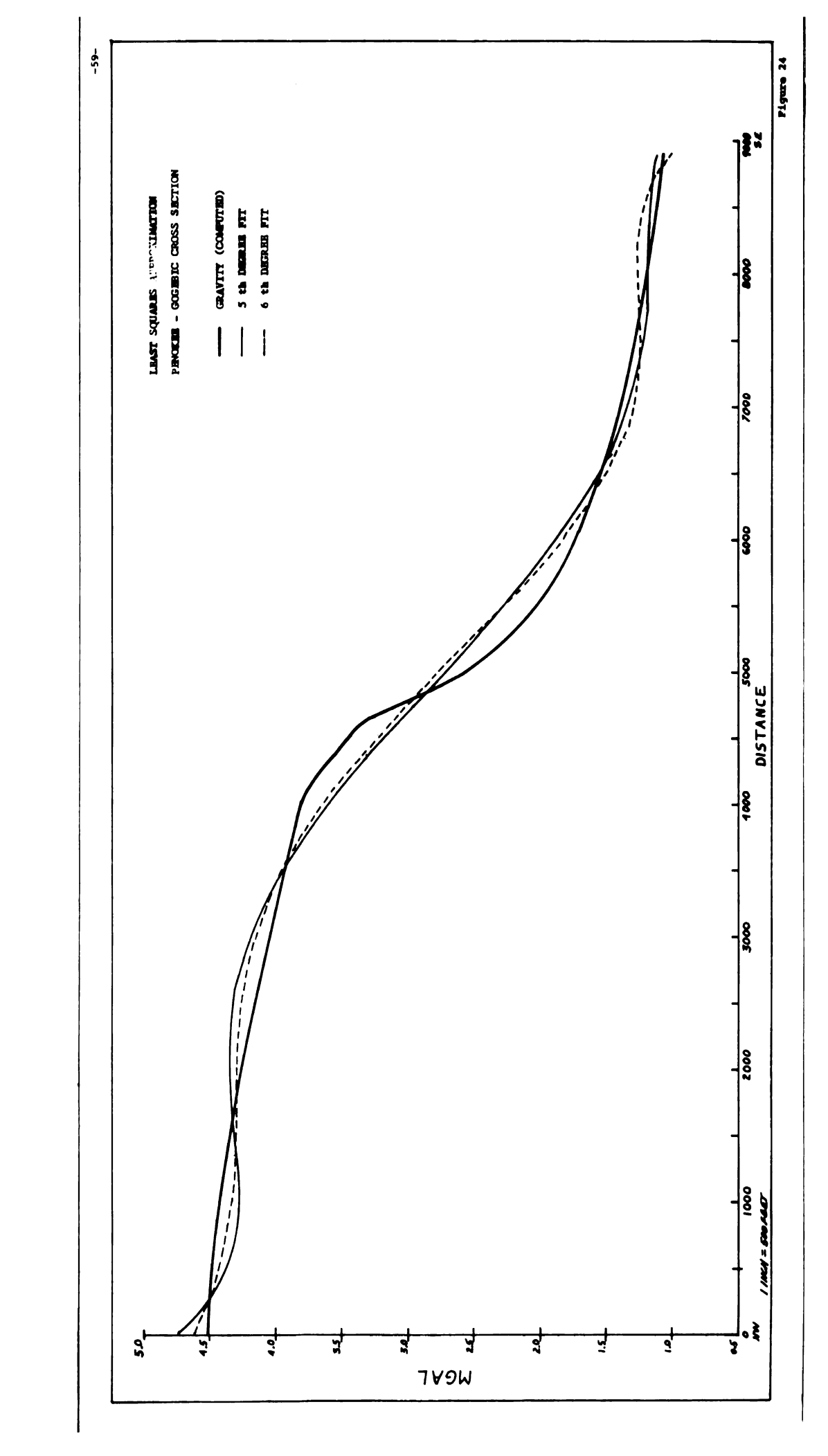
yield widths of about 250 to 260 feet for the iron formation, compared to an actual width of 200 feet.

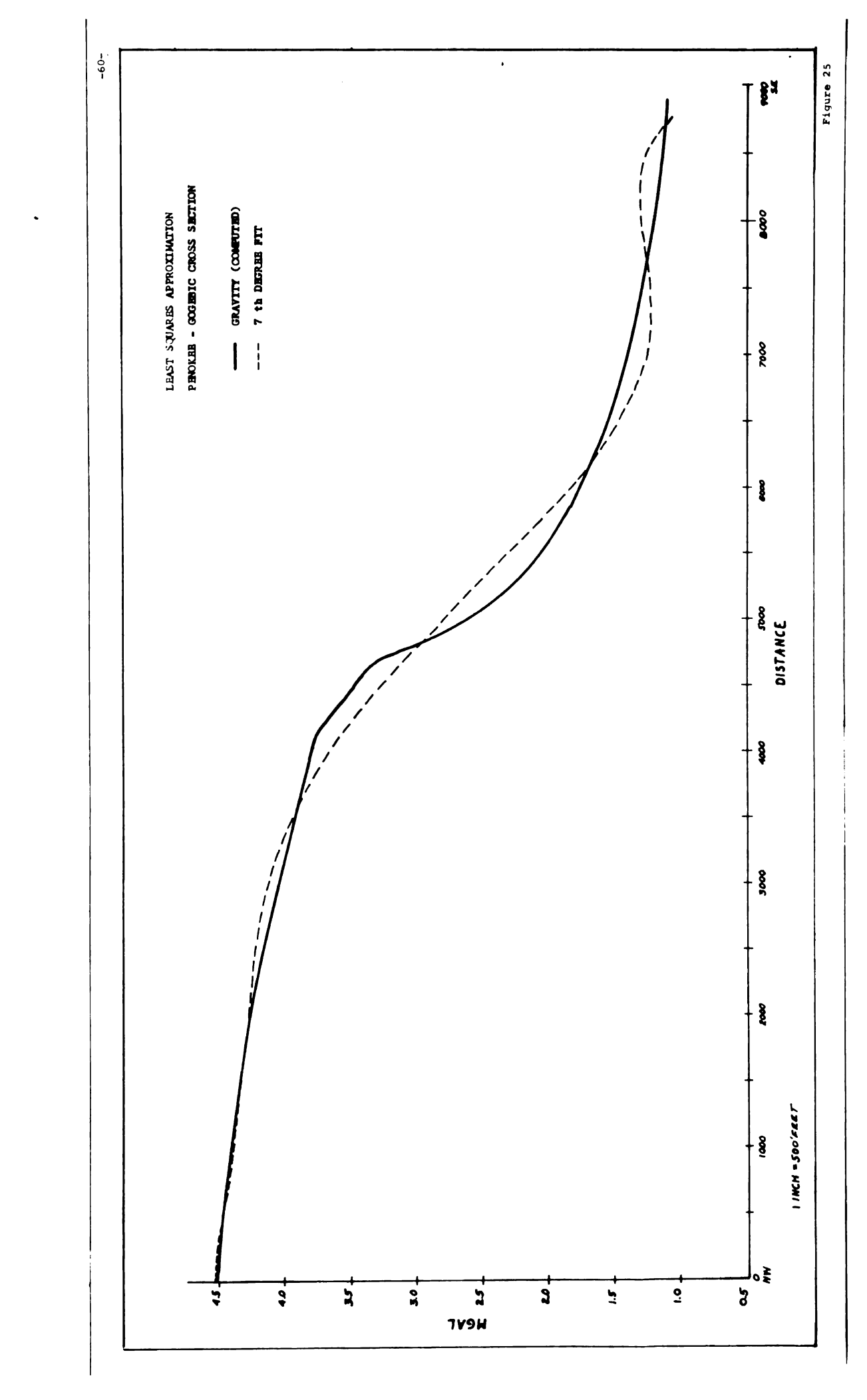
Smooth Curve Interpretation. The smooth curve estimation of the region appears in Figure 28. The residual anomaly which remains, isolates a rather broad flattened anomaly much the same as the least squares approximations using the higher degree fits.

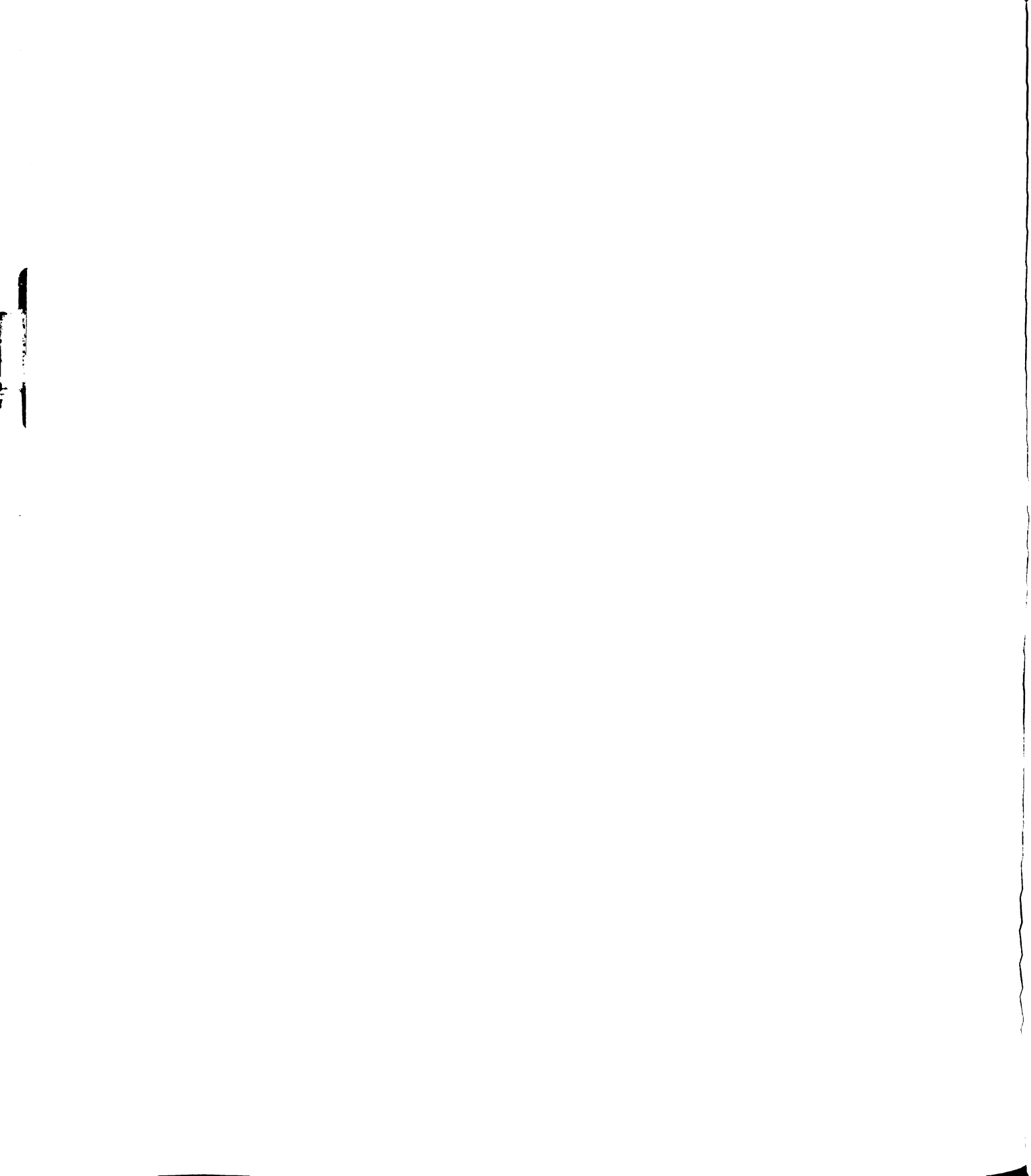
Least Squares Approximation. In order to show the successive approximations by the least squares method, the curves for approximating polynomials from the 1st to the 10th degree are shown in Figure 23 to 28. In addition to the 10th degree approximations, the 18th degree is also shown. At the conclusion of this study a new and much larger digital computer, the Control Data 3600, was being installed at Michigan State University. While the computer was still in the testing and acceptance stages, one least squares program was accepted on a trial basis and the partial results are included in this paper to indicate that higher degree polynomials can be obtained with larger digital equipment. The curve is shown in Figure 30.

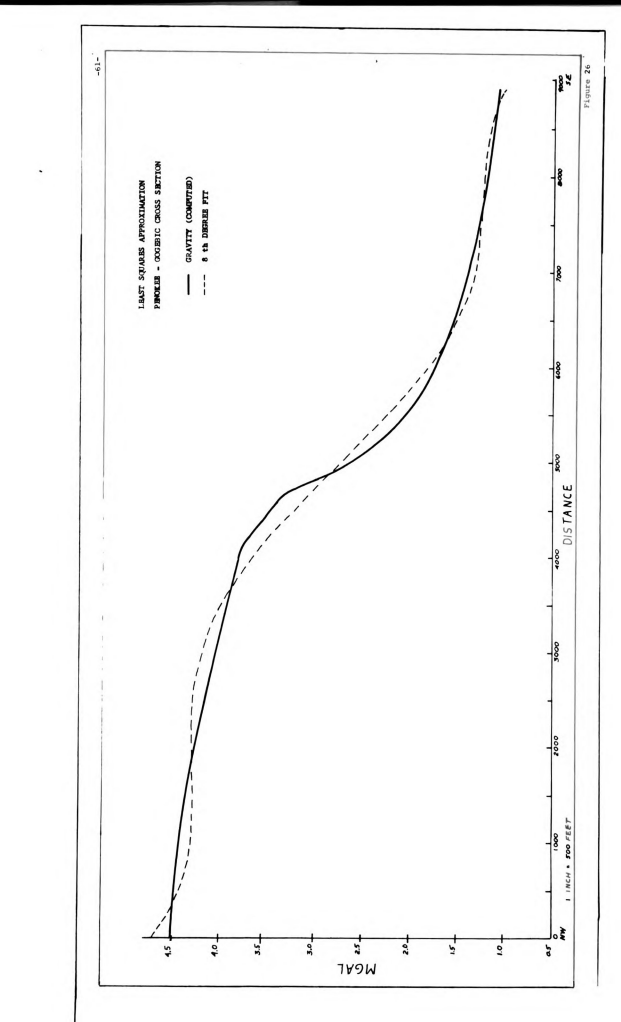
With regard to the curves for the 1st to the 10th degree approximations, it should be noted that there is only slight

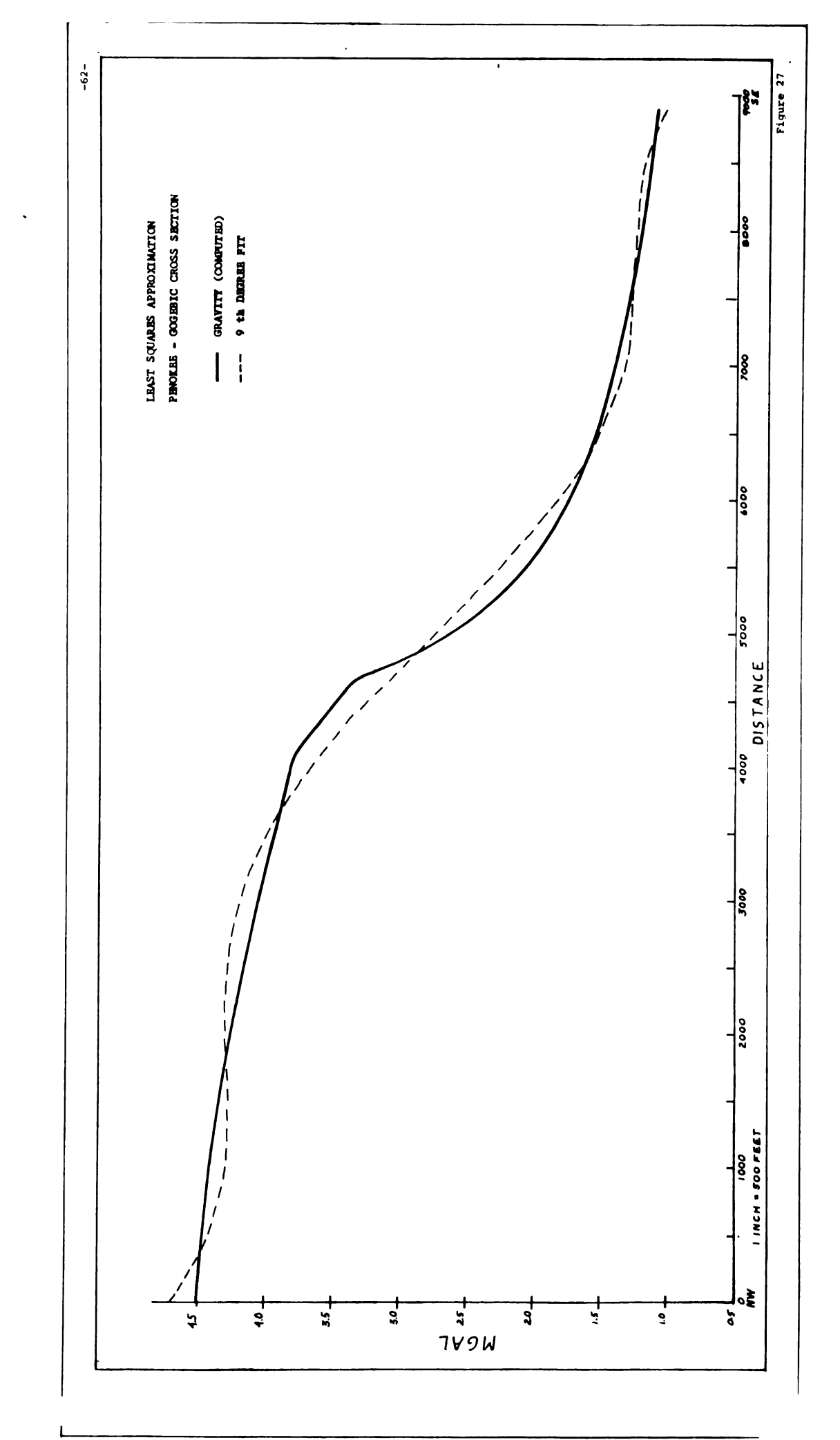


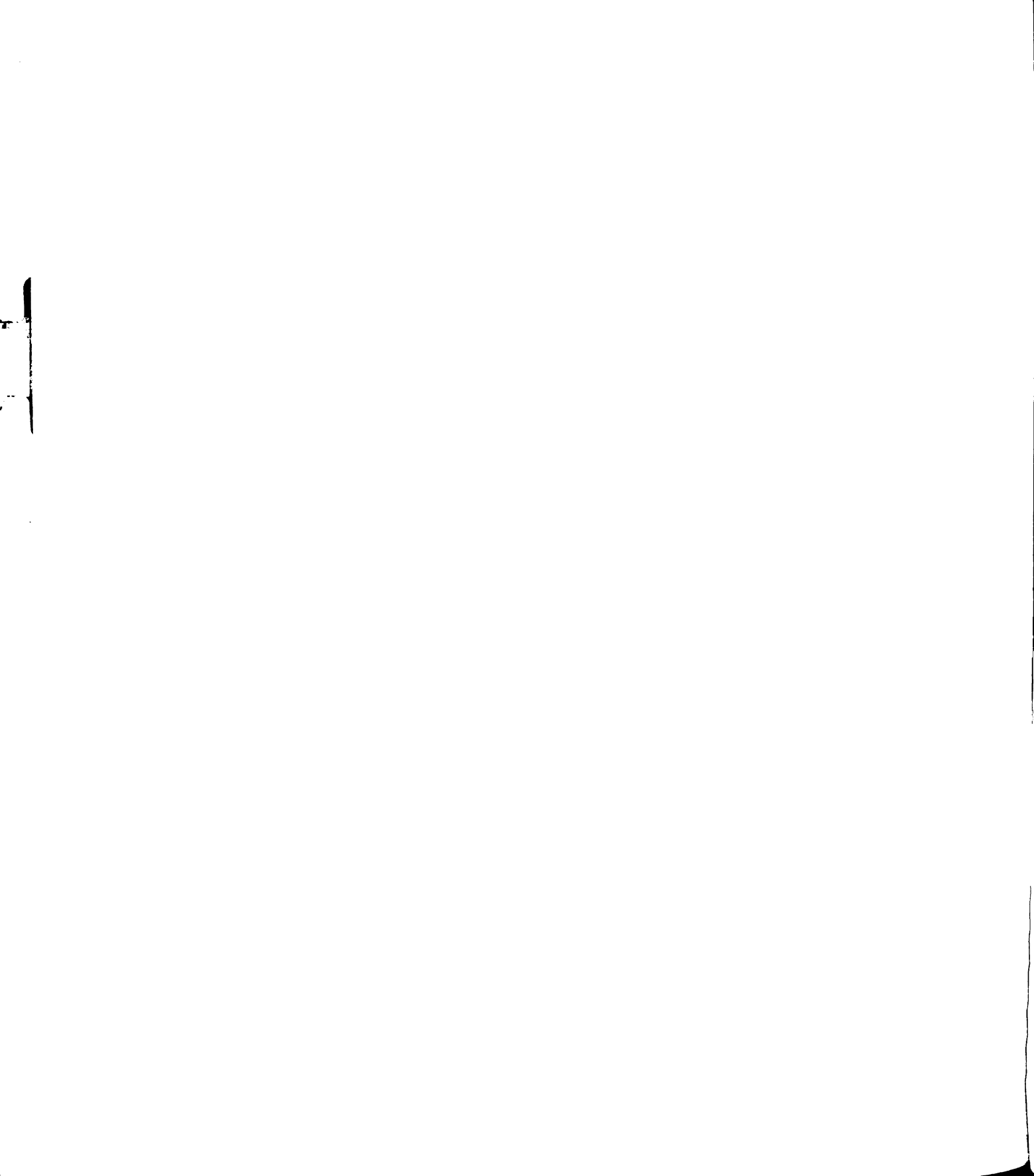


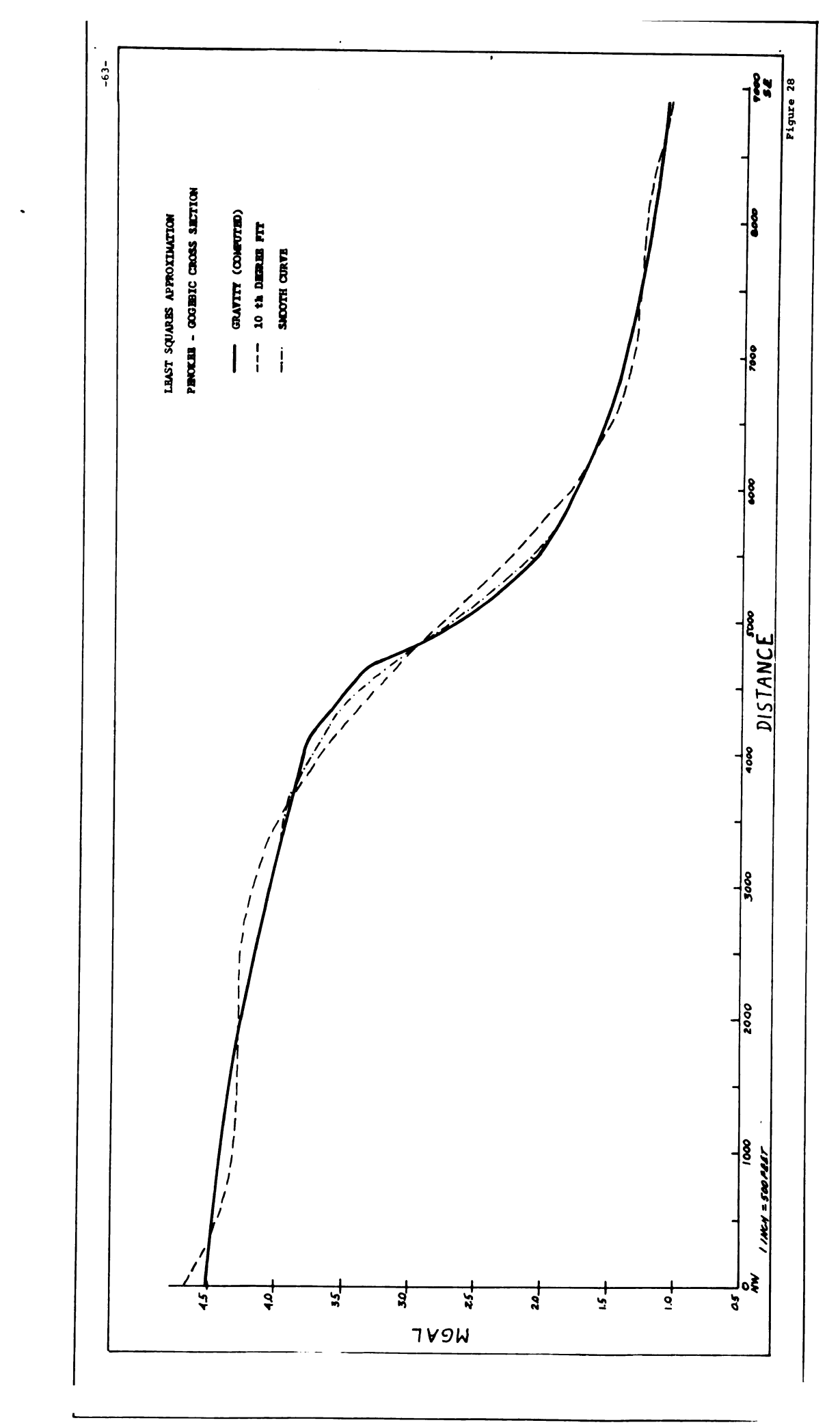


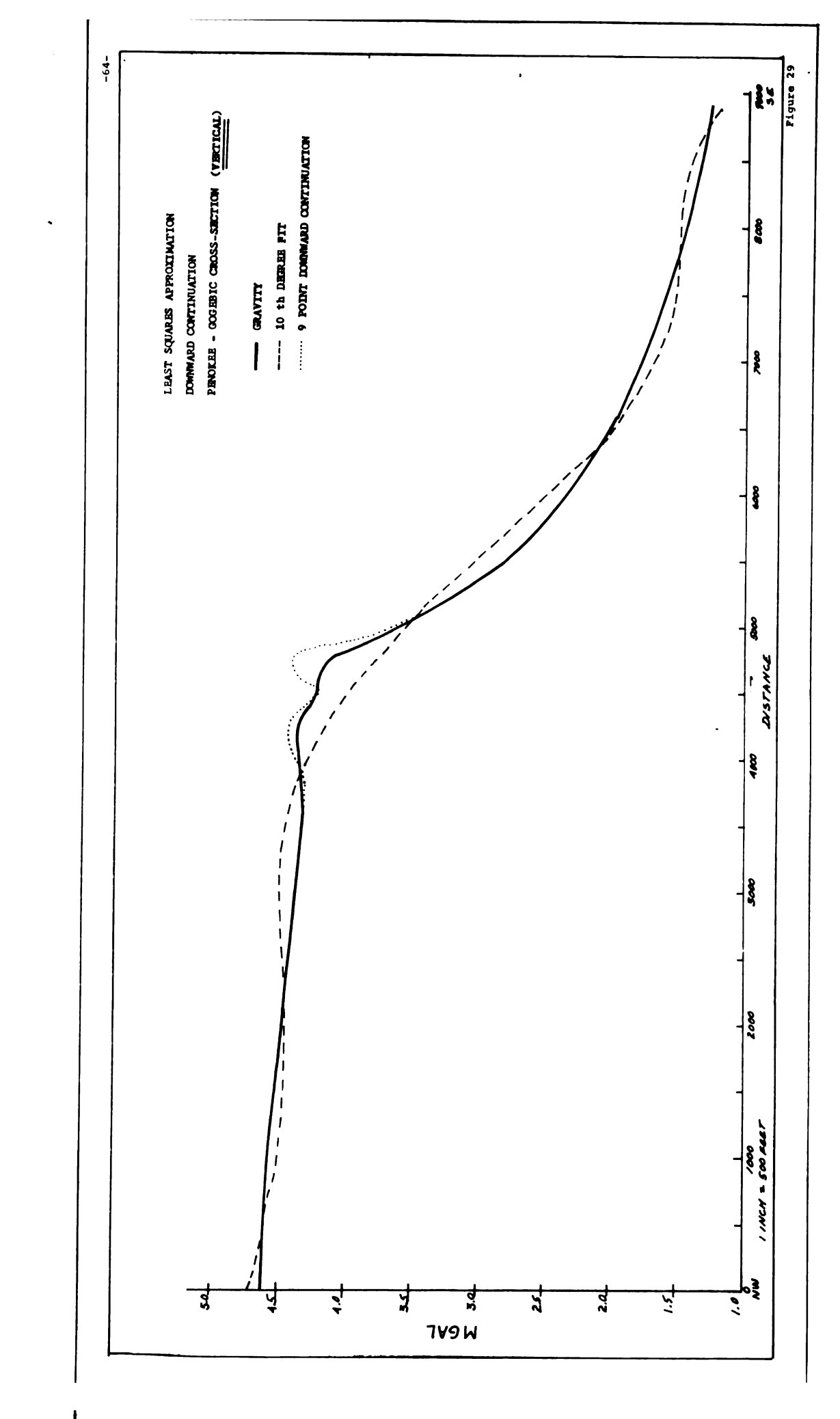


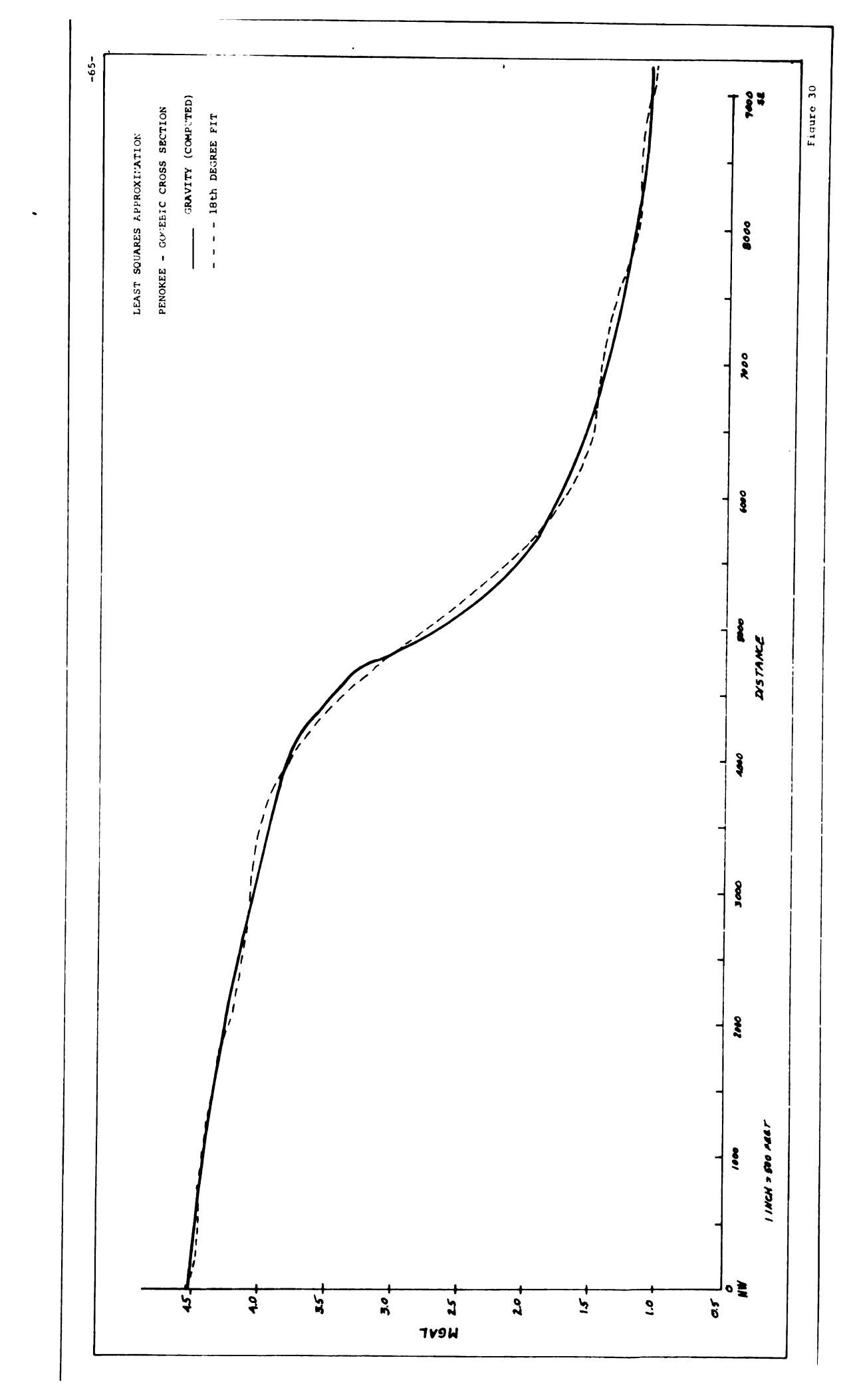


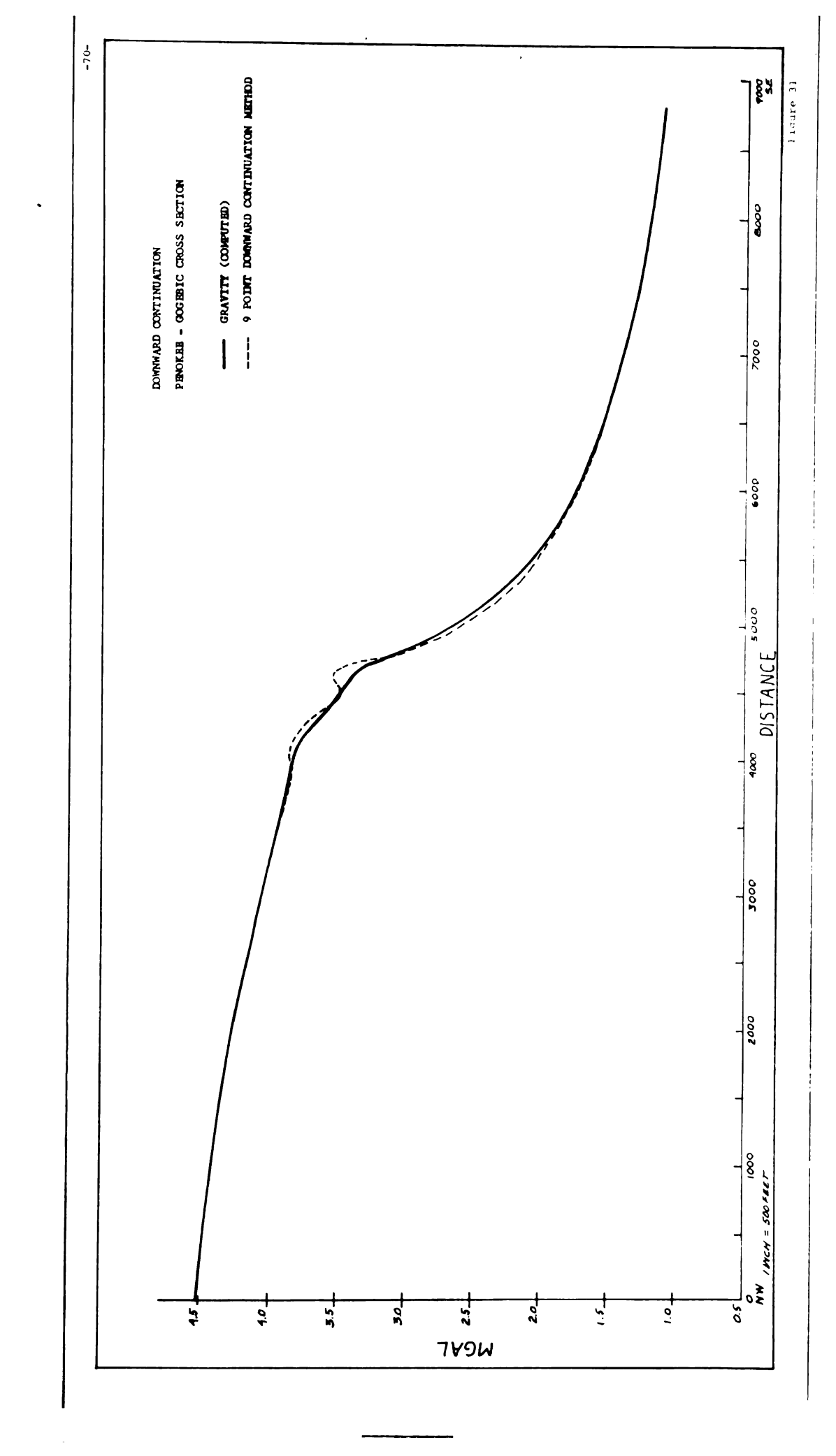












visible difference between the 7th, 8th, 9th, and 10th degree approximations; however, the Table 1, page 34, indicates there is a change in the $R(x)^2$ value.

Downward Continuation Interpretation. The curve in Figure 34 is the nine-point downward continuation of the Penokee-Gogebic gravity profile. Shown in Figure 29 are the results of the method as applied to the Penokee-Gogebic cross-section when it is assumed to be vertical. Figure 31 illustrates the downward continuation method applied to the profile when it is assumed dipping. The nine-point downward continuation was used to continue the curve down 100 feet.

OBSERVED GRAVITY PROFILES

The two observed gravity profiles used in this study were obtained from the Jones and Laughlin Steel Company.

The first profile is believed to cross the Magnetic Center iron formation, and is located on the Marenisco range, Iron County, Wisconsin. Beutner (1958) and Hinze (1960) describe the area. An east-west linear-type iron formation with a thickness of over 1,000 feet dips to the south at approximately

65°. The iron formation is bounded to the north and south by chlorite schists. Overburden is estimated to be about 70 feet as determined by seismic refraction studies and drilling. The profile used in this study is located about 9,600 feet west of the area just described. It is believed that the profile does cross an iron formation.

The second gravity profile is located in Canada, approximately 100 miles east of Rainy Lake, Ontario. The profile is over the Bending Lake iron formation. The iron formation, occurring in a series of schists, consists of alternating bands of quartz and magnetite. Quartz-biotite schist and garnet schist are suggested from drilling and outcrops. Previous study of the area (Hinze, 1960) suggests a southwest dipping linear iron formation with a width of 1,000 feet. Hinze calculated a theoretical gravity profile over the iron formation and was able to obtain close correspondence with the observed profile. A linear dipping formation was assumed having a depth of 4,000 feet. The upper 1,000 feet is made up of an iron-rich formation and quartz-biotite schist, in alternating bands. The lower 3,000 feet are made up of material of lower density.

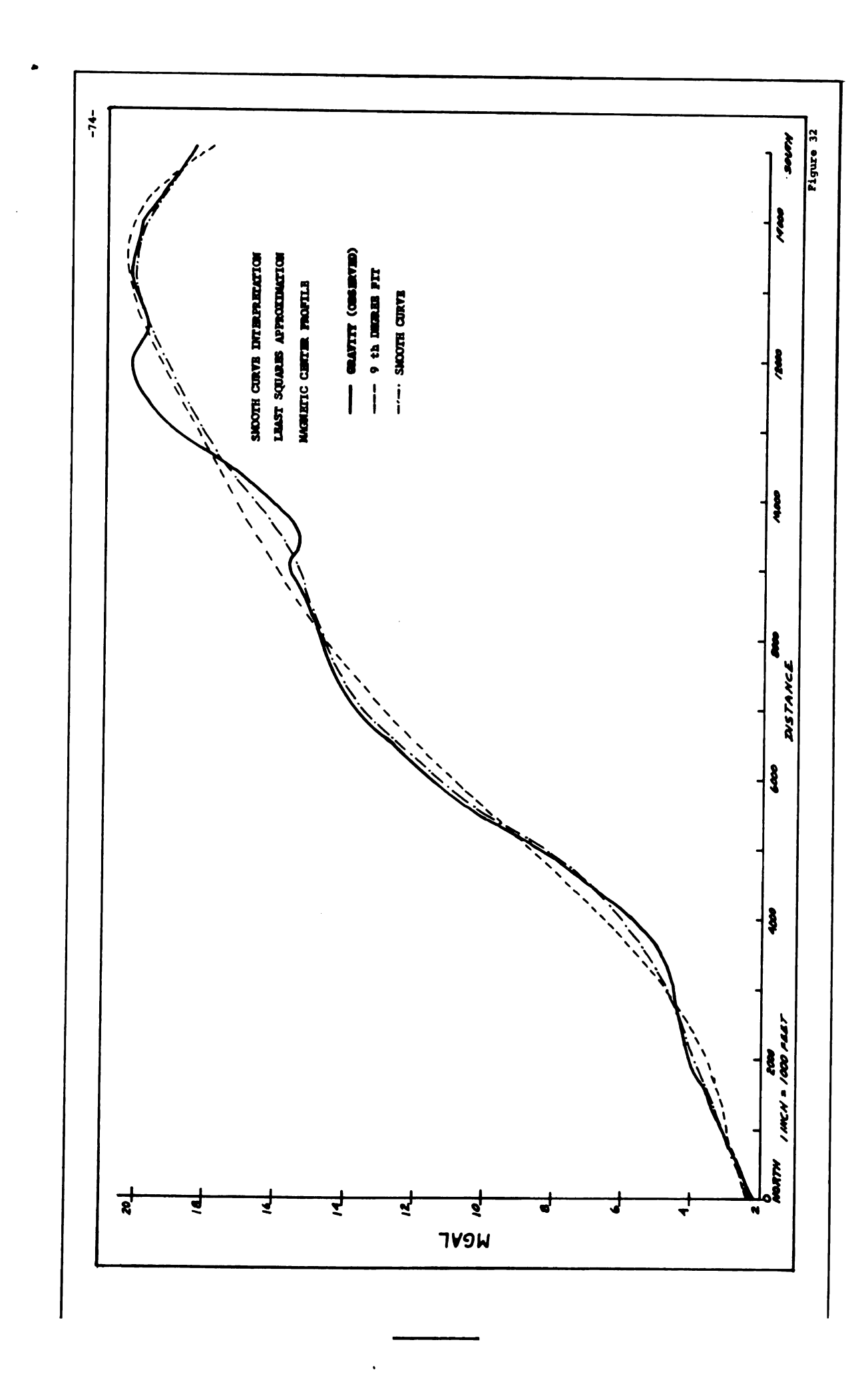
Magnetic Center Interpretation

General Discussion. The gravity profile as shown in Figure 32 along with the smooth curve estimate of the regional reveals the Magnetic Center anomaly is complex and no really clear outline of a residual is seen. Geologic information can only be extrapolated from the known area to the east, the nearest drill hole being about 5,000 feet away.

The profile is 16,400 feet long with a station spacing of 200 feet. Equal station spacing was obtained by interpolation between values.

Smooth Curve Interpretation. Shown in Figure 32 is the smooth curve estimate of the regional anomaly over Magnetic Center. The resulting residual anomaly is located at the west end of the profile. Actually two anomalies close together are the result. Interpretation of the widths at which the smooth curve approaches the gravity profile gives a width of one residual of about 800 feet, plus another narrower anomaly at the end of the profile of about 700 feet.

Least Squares Approximation. Figure 32 also shows the 9th degree least squares approximation of the Magnetic Center anomaly. However, this method produces a residual whose width



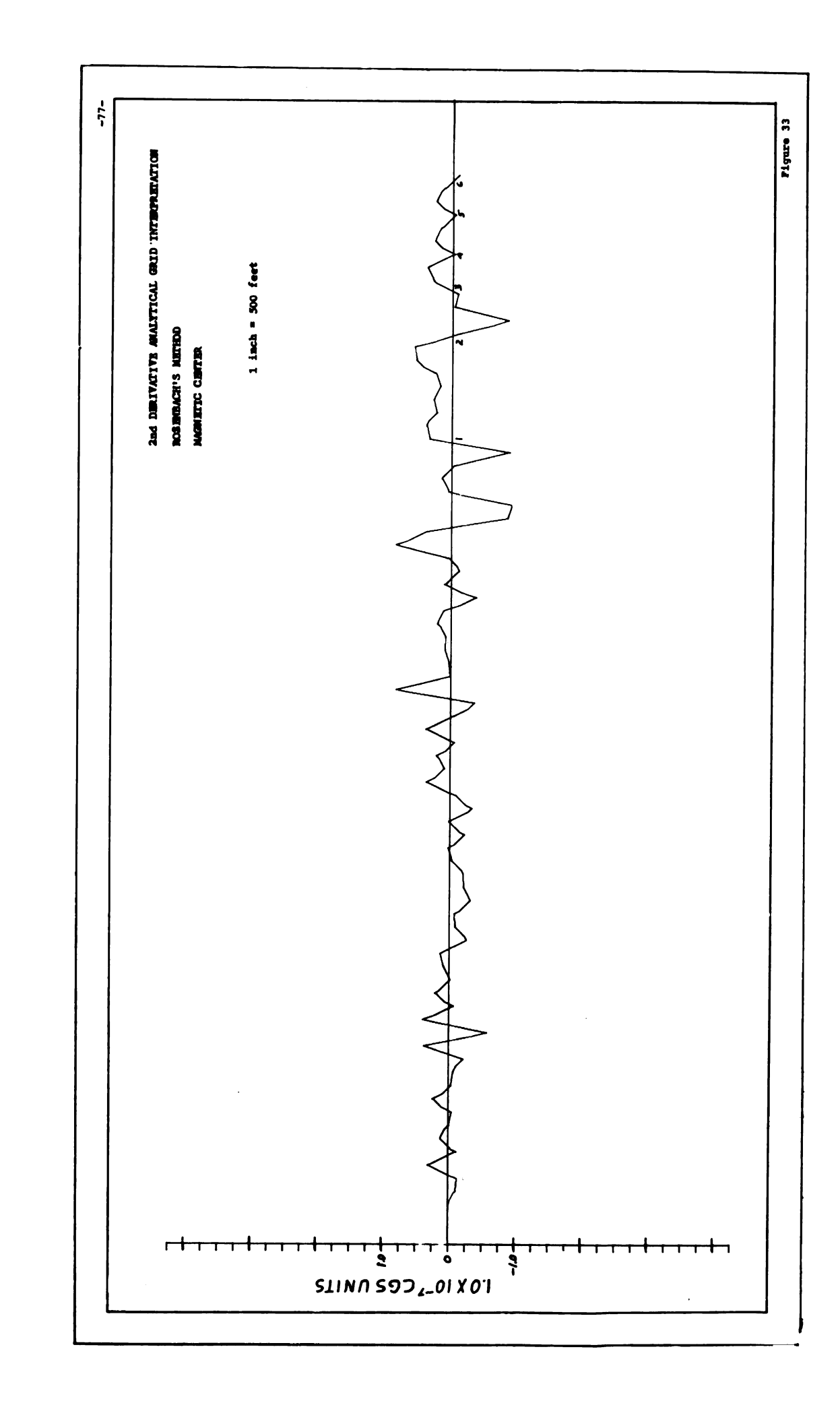
at the base is approximately 1,000 feet wide, and eliminates the second minor anomaly isolated by the smooth curve method. The 9th degree fit also yields a rather predominant negative residual to the north of the residual anomaly. This low was also exposed by the smooth curve method.

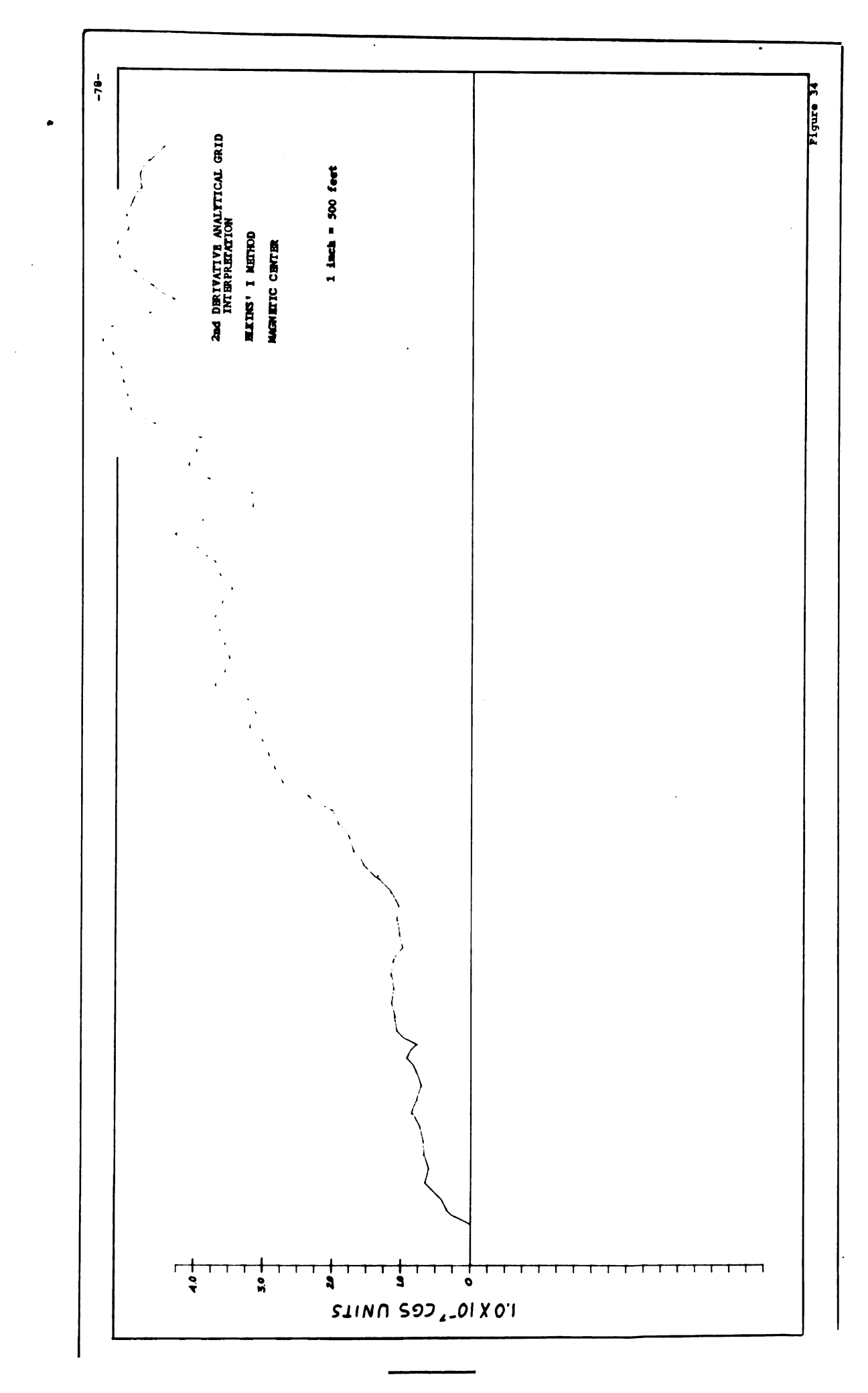
and Derivative and Empirical Grid Interpretations. A major difficulty in the use of 2nd derivative method when applied to actual gravity data is the effect of random error and small variations in gravity. The method, because of its high resolving power, is very sensitive to these small variations in gravity data. When these variations are analyzed with the 2nd derivative method, the resulting anomalies can be mistaken for real anomalies associated with structure or density changes. The resultant 2nd derivative curve, therefore, contains anomalies which appear natural but may be completely irrelevant. Elkins (1952) has written a paper dealing with the subject and derives statistical measures for estimating the correlation between 2nd derivative values and also the probable error associated with these values.

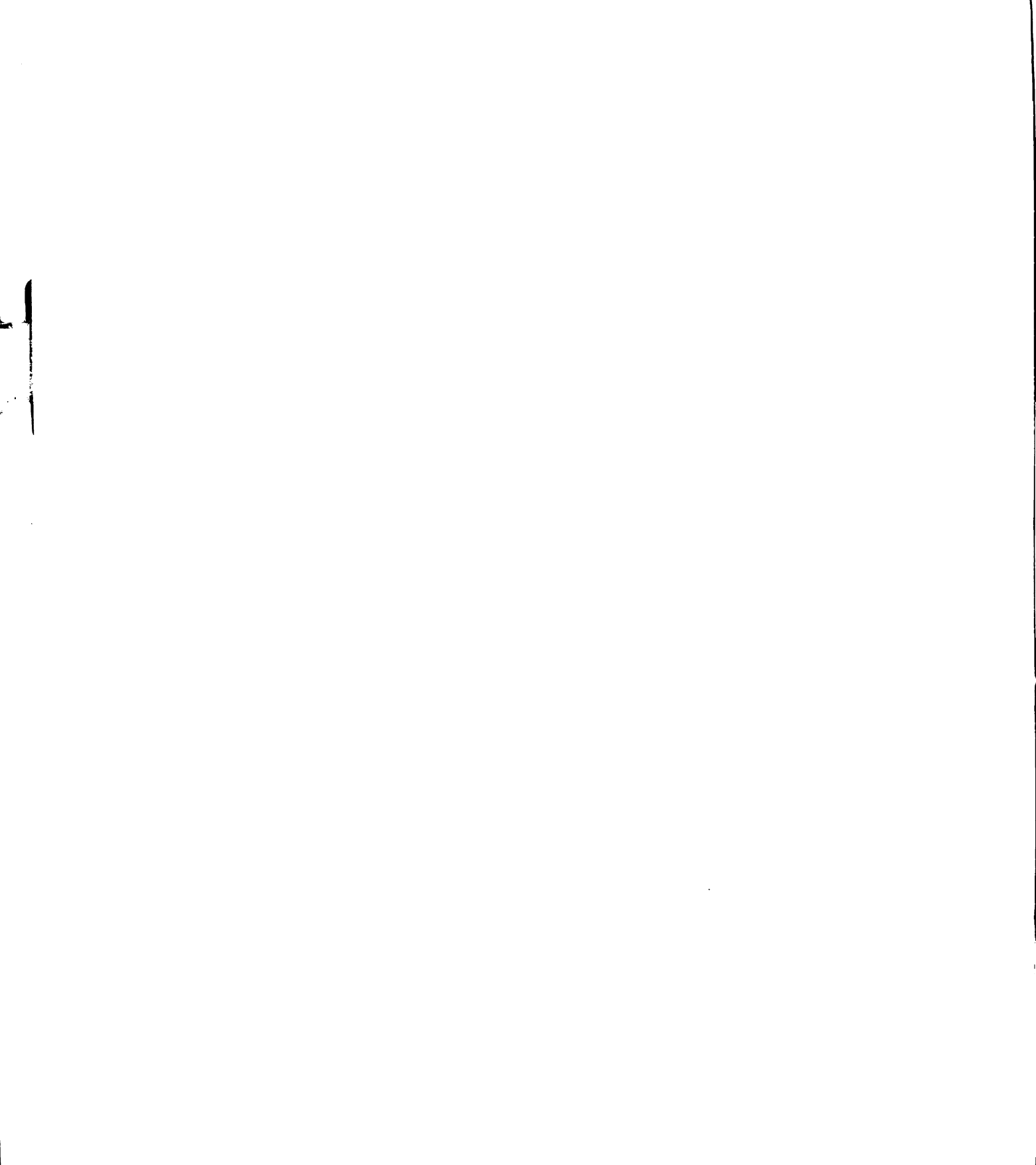
The profiles shown in Figures 33 and 34 are the resultant curves from Rosenbach and Elkins' I method.

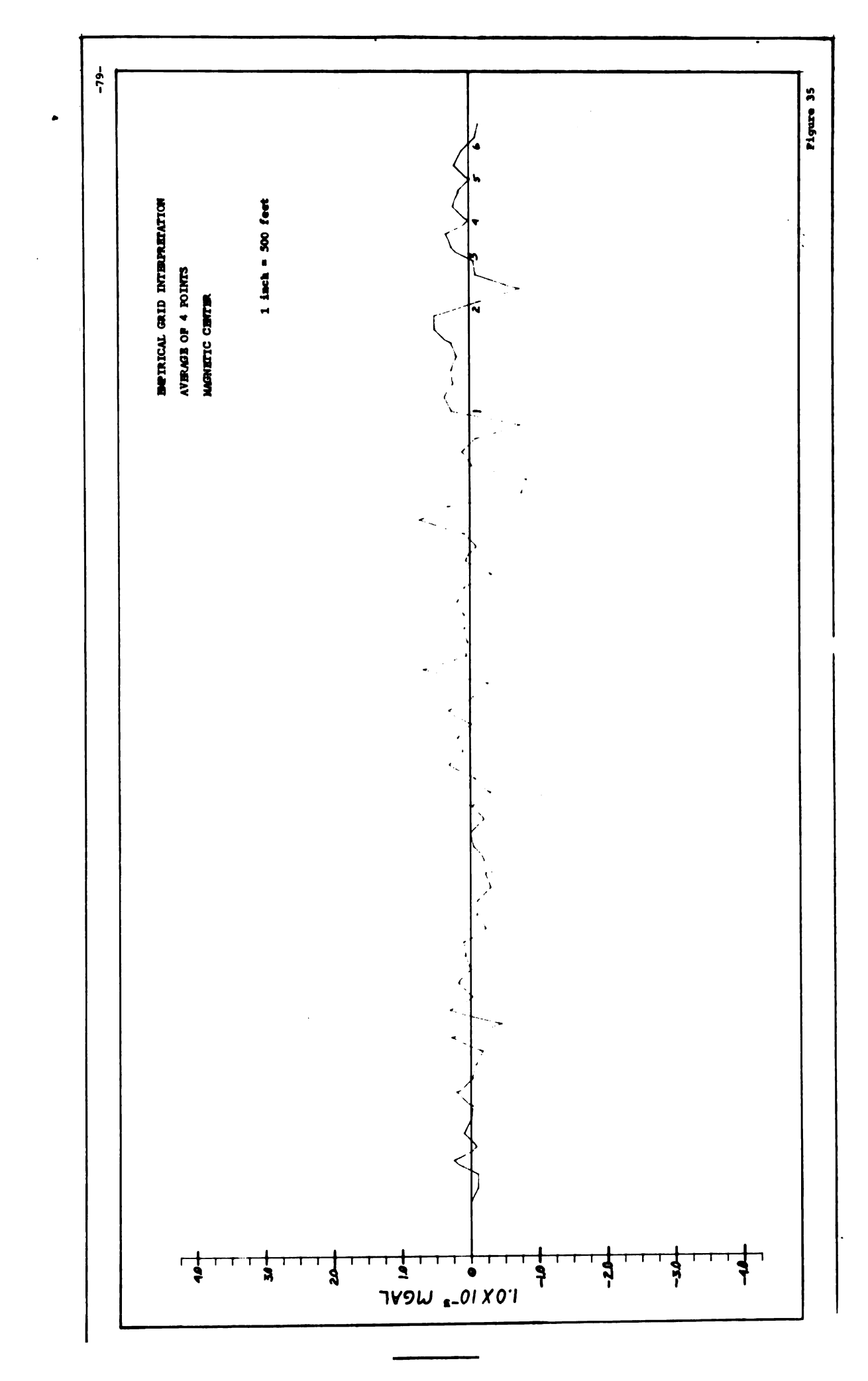
Rosenbach's method results in a profile that is hard to resolve. So much of the curve is reduced to plain "noise" that it is difficult to isolate the true anomaly. However, some valid information may be gained by looking at the points where the curve crosses the zero line of the axis at the south end of the profile. These have been numbered 1, 2, 3, 4, 5, These points could be interpreted as points which represent physical limits on various widths of the alternating bands of magnetite rich horizons within the iron formation. would yield from 1 to 2, a width of about 810 feet of iron-rich material. From point 2 to 3 the curve cuts the zero line giving a width of about 300 feet; this could be interpreted as being material less rich in iron content. Points 3 to 4, 4 to 5, and 5 to 6 all measure roughly 150 feet apart and could represent successive layers of iron-rich material. However, points 3, 4, 5, and 6 do not cross the zero line and become negative, so some caution should be used with these points.

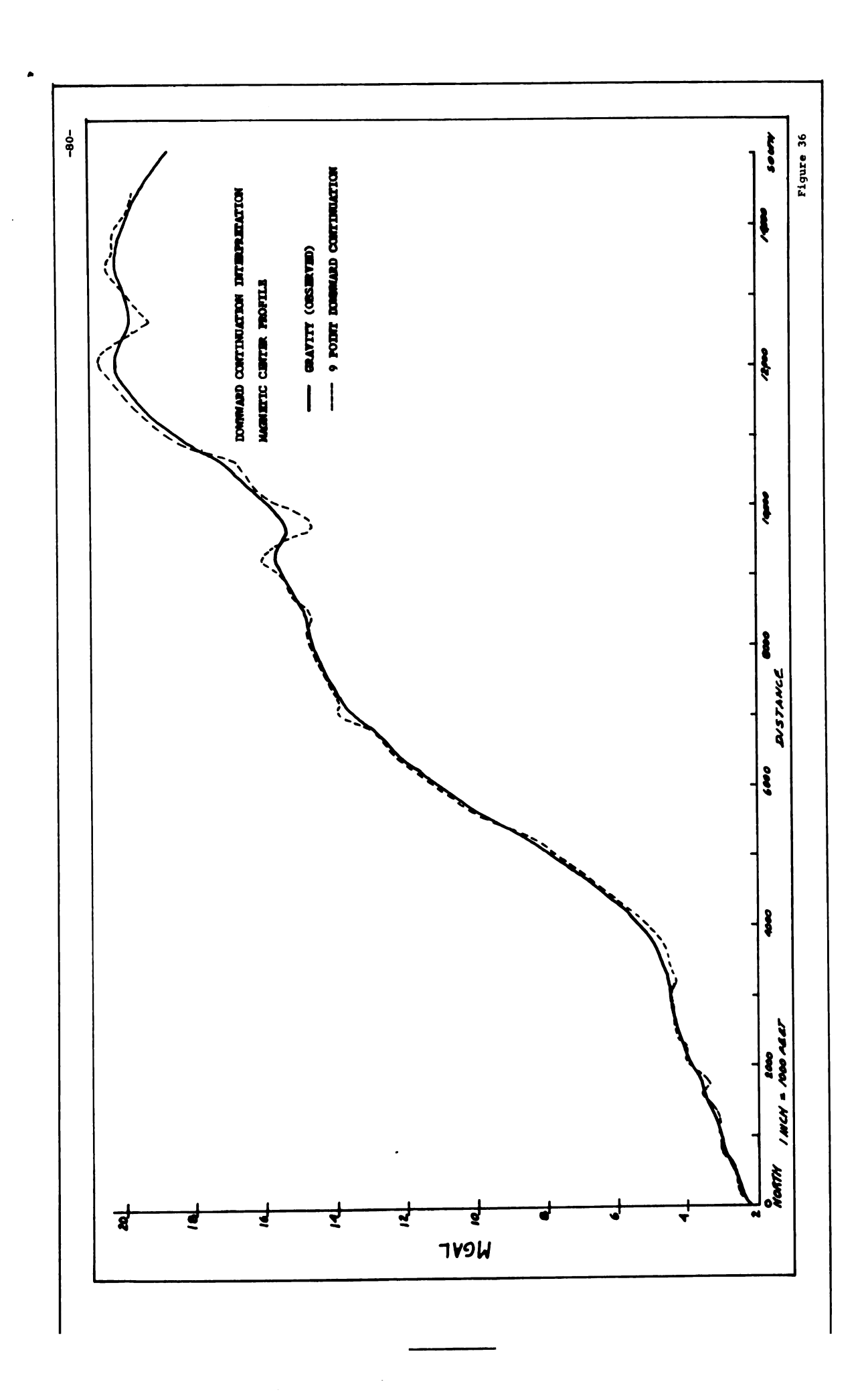
The empirical grid method, as shown in Figure 35, also gives the same quality of data and could be interpreted in the same manner. Elkins' method gives the same general outline as the original gravity profile but with some resolution and isolation of the anomalies.











Downward Continuation. The nine-point downward continuation interpretation as shown in Figure 36 leaves little doubt as to the location of the major anomalous areas. The small northerly residual which has been eliminated by the least squares method is isolated, but is of low magnitude and appears to have less significance than the major residual immediately to the south. The center point of the negative anomaly is well placed by this method also.

Bending Lake

General Discussion. The Bending Lake anomaly is much more predominant, in regard to recognition, than that of the anomaly over Magnetic Center. The profile has had some preliminary smoothing of the original data to permit better utilization of the analytical grids and empirical grids. Preliminary smoothing is defined as the removal of the more obvious errors and "noise" in observed gravity data. The estimated residual has a magnitude of about 1.0 mgal. Also shown is a minor residual at the southwest end of the profile. This could possibly be attributed to a dike or some other type of intrusive body.

Smooth Curve Interpretation and Least Squares Approximation.

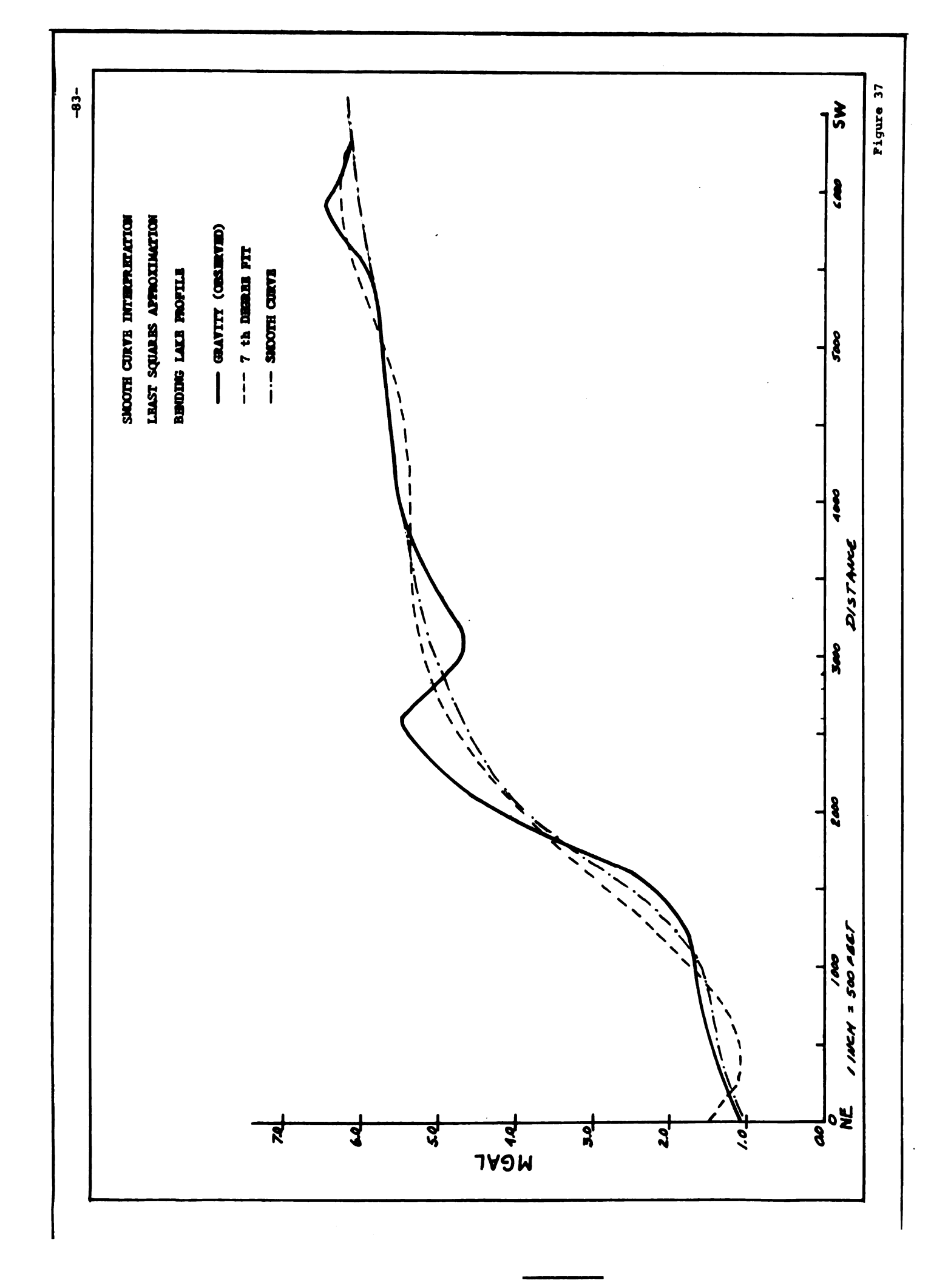
Shown in Figure 37 are the two different estimations of the

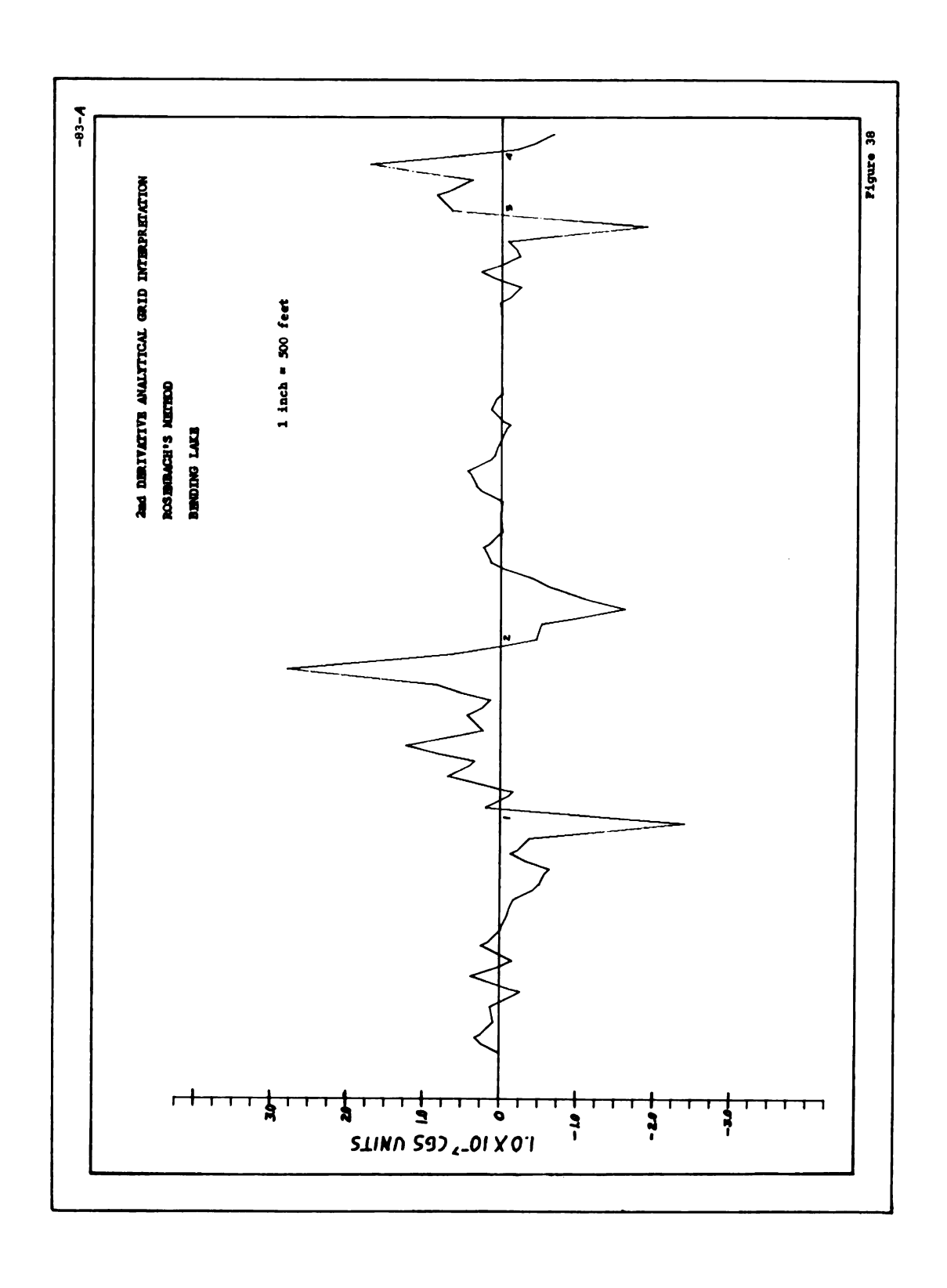
regional anomaly. The smooth curve, perhaps guided somewhat by experience with the profile of the Michigamme Mountain, produces a residual anomaly whose width at the base is almost 1,000 feet. The least squares method produces a residual whose width at the base is approximately 900 feet.

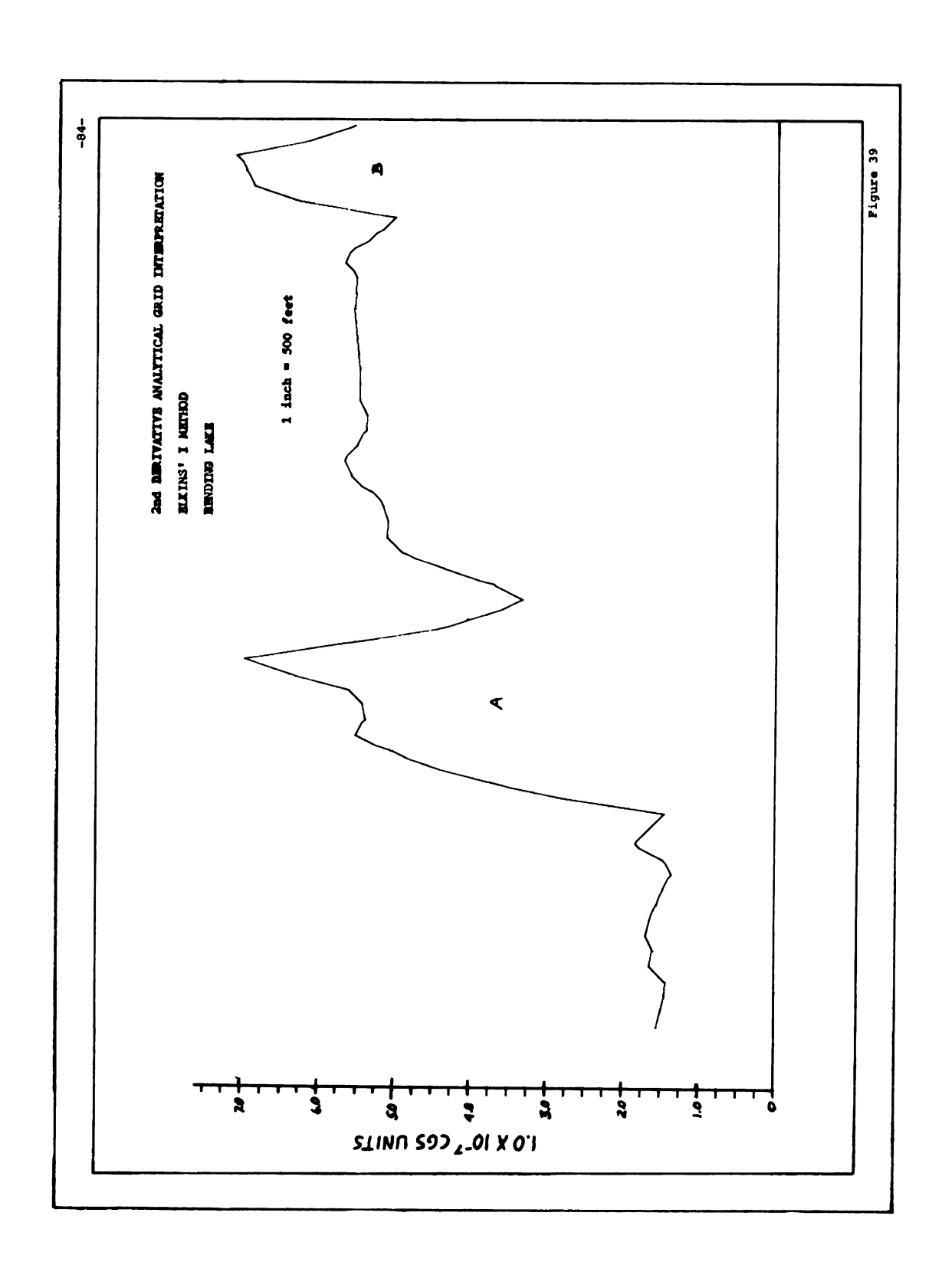
In this particular case, the smooth curve estimate appears to give a better estimate of the regional than does the least squares approximation. The least squares 7th degree fit tends to weave in and out between the original gravity profile.

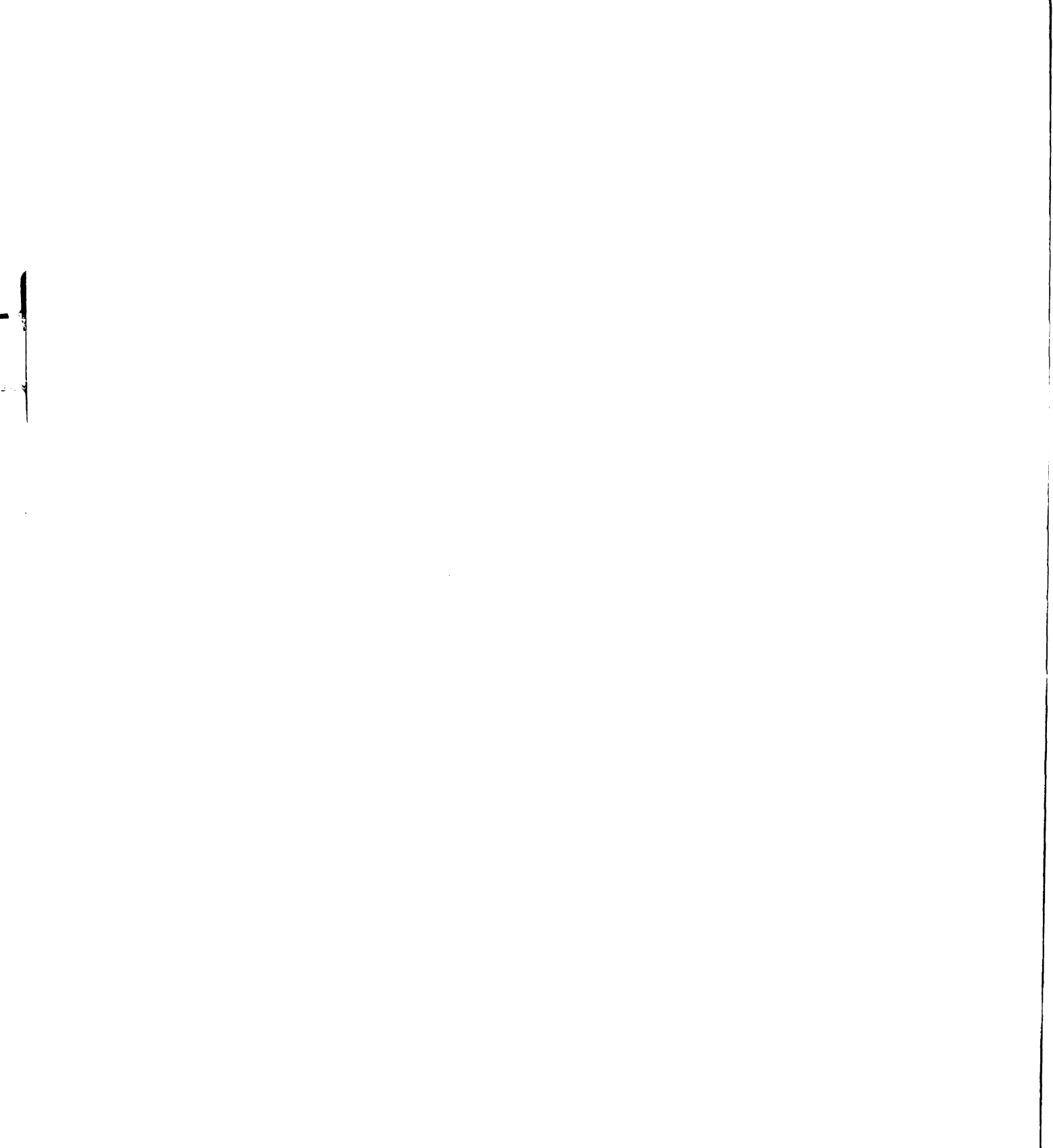
2nd Derivative and Empirical Grid Interpretations. The two analytical grid methods used on this profile were Rosenbach's and Elkins' I. The Figures 38 and 39 represent reproductions of the 2nd derivative profiles as plotted by the digital incremental plotter. Approximately two minutes were required to compute and plot each of the curves, utilizing the computer.

Figure 38 represents the profile using Rosenbach's method. The plot does contain four points which may correlate with the two anomalous areas of the gravity profile. The first anomaly gives a width at the zero line of 1,050 feet, (measured from point 1 to point 2, Figure 38). This is a reasonable figure since the original estimate of the iron formation from drilling was 1,000 feet. The second anomaly at the southwest end









of the profile produces a width of about 410 feet, (measured from point 3 to point 4).

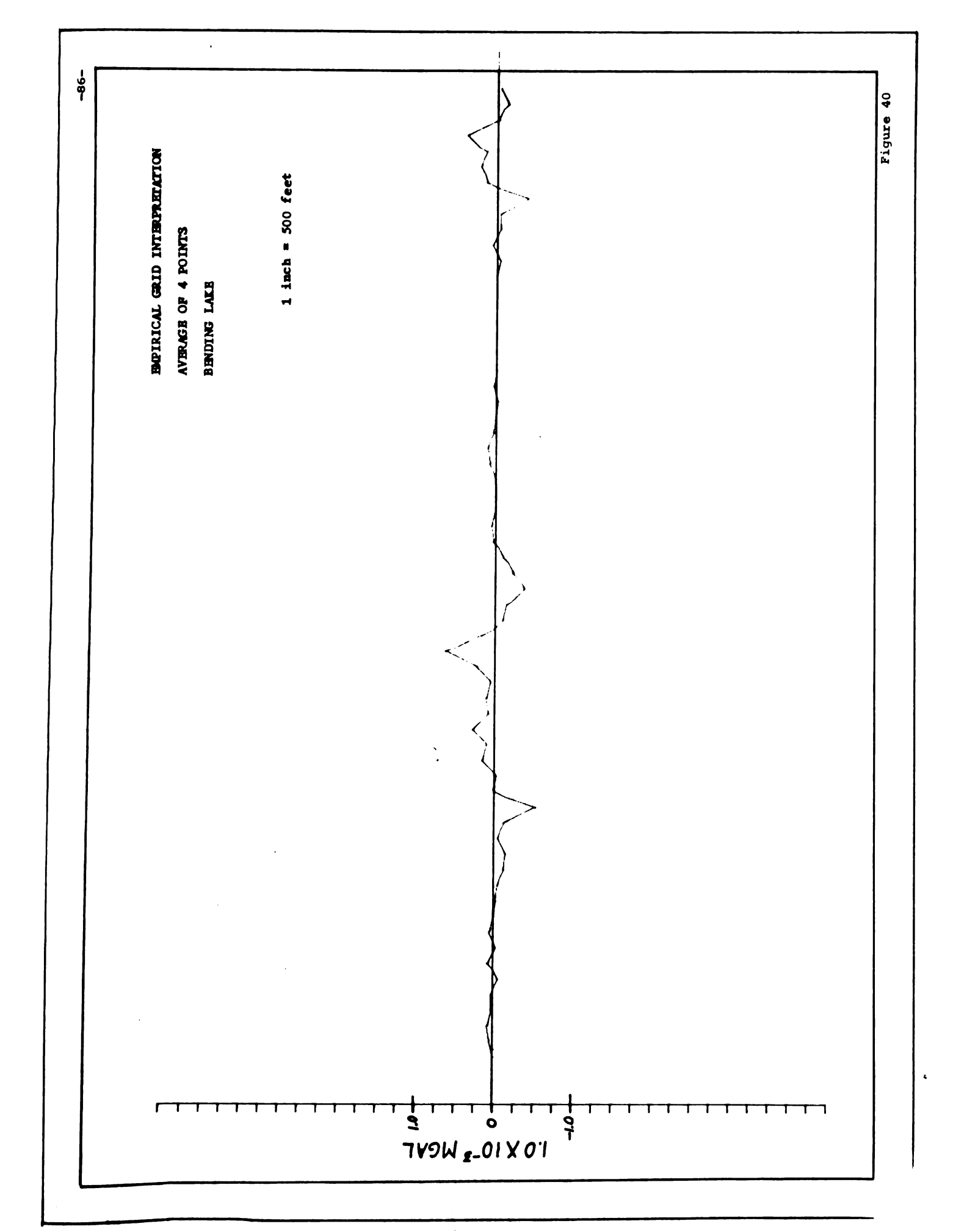
Elkins' I method as shown in Figure 39 gives much less information about width of the formation causing the anomaly. However, the method does outline and isolate the anomalies quite well. The two major anomalies are labelled (A) and (B).

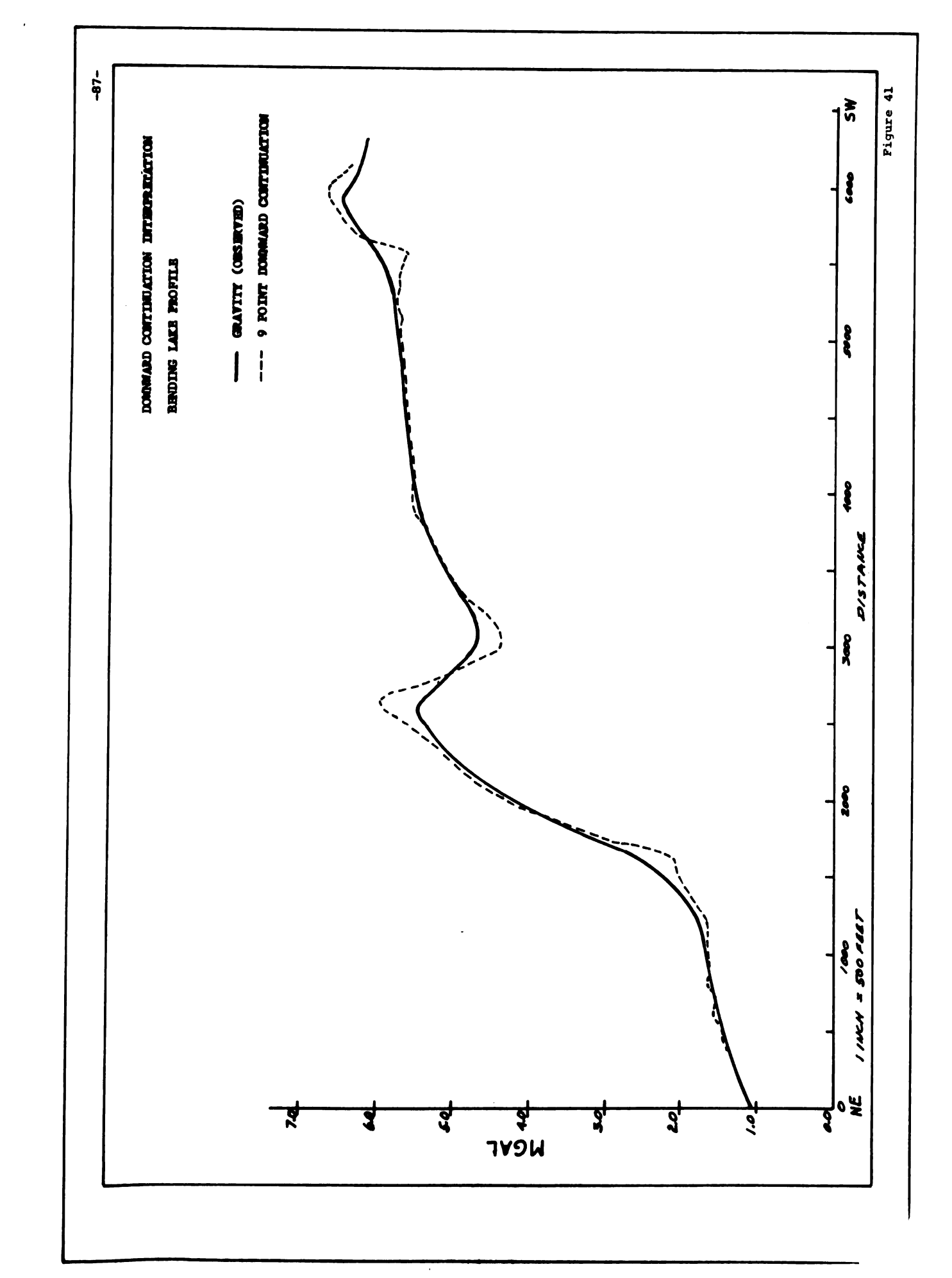
The empirical grid method is shown in Figure 40. However, analysis of the curve as it crosses the zero line yields the same widths as Rosenbach's method, that of 1,050 feet for anomaly (A) and 410 feet for anomaly (B).

Downward Continuation Interpretation. The nine-point downward continuation method shown in Figure 41, as in other profiles, clearly isolates the major anomalous areas on the profile.

The method also isolates clearly the negative anomaly immediately to the southwest of the major positive anomaly.

Using computer techniques, the method of downward continuation requires about two minutes to compute and plot on the digital computer.





CONCLUSIONS

The review of various methods of treating the regional effects and of isolating local anomalies shows there is no single direct answer to the problem. However, some definite conclusions can be reached as to which of the methods used in this study are most ameanable to the problem at hand.

It must be conceded that the effectiveness of these methods in prospecting is limited by the inability of any one method to make an exact interpretation of the data. The responsibility for this can be placed upon the inherent ambiguity of potential field interpretation.

The specific problem, that of separating a local anomalous field from a regional background with an extremely high gradient, makes the basic assumption that one knows what the residual is. Another equally important assumption is that details are known about the geology to the extent that it provides means of judging what the regional is. It is, therefore, apparent that one of the most critical parts of interpretation of gravity data is the assigning of separate causes to separate effects; and as Nettleton (1954) states,

"The problem of regionals and residuals arises in all geophysical methods which are based on measurement of a potential field . .

. . . Basically, the question is that of separating a potential field into possible component parts and of ascribing separate geologic causes to these parts."

The one basic criterion that is needed is considerable geologic background from which to draw.

Of the methods used in this study, smooth curving is perhaps the one method in which personal judgment plays a major role in the isolation of a residual anomaly. All other methods systematize the process with some method of mathematics or logic, and reduce personal judgment to a minimum.

A critical review of the methods reveals certain properties inherent in each method. As mentioned above, the method of smooth curves is a matter of personal judgment, and where the smooth curve coincides, the regional is left purely up to the individual. The individual's background, experience, and intuitive feel for the data may or may not yield the desired results.

The method of least squares is an excellent example of how personal judgment is almost completely removed from the individual determining the regional. The method of least squares will consistantly give, at its worst, a rough esti-

mate of the regional anomaly. The higher the degree fitting polynomial will generally yield data which approaches the original gravity values. A basic estimate of the effectiveness of the method is the value of the error term, $R(x)^2$. Generally speaking, a 10th degree polynomial will give a relatively good approximation of the regional anomaly. It is not safe to make any qualitative judgment on the magnitude of the resulting residual or to make width determinations based on the resulting residual anomaly. It is possible to obtain polynomials of a very high degree, but it does not give enough information to warrant the cost of computer time.

The use of the empirical grid produced results consistently equal in quality with that of the analytical grids. As applied to theoretical data, the method gives a good estimate of the width of the causitive body. In terms of ease of computation, the method is superior to the analytical grids. While only one method, the average of four points about a circle was used, other figures may produce the same or better results. As applied to observed gravity data, the method produced the same width estimates as Rosenbach's analytical grid.

In using analytical 2nd derivative grids, the use of seven different methods resulted in actually only two interpretations.

The methods of Rosenbach, Elkins II, McCollum, Haalck, and Henderson and Zietz give equal width estimates, with the only variations being that of amplitude of the produced 2nd derivative anomaly. Elkins' I method gives very poor estimates of widths, but does reproduce in general outline the original gravity data with the anomalous areas well isolated.

The 2nd derivative method has such high resolution that when the method is used with observed gravity data of average precision and with normal variations in gravity, it produces false anomalies which are frequently mistaken for actual residual anomalies.

The method of downward continuation produced consistently good results, always isolating the residuals and only slightly emphasizing the larger regional type structures. The difference between the five-point and nine-point downward continuation is very slight. The advantages gained by use of the nine-point do not seem to call for its use in hand computation, whereas with computer usage it makes little difference.

In summary, the method of downward continuation, empirical and analytical 2nd derivative grids seem to give the best results for making interpretation of gravity data. The grid methods, while being very powerful, are very sensitive to minor variations in gravity data and may create superficial anomalies.

The method of least squares, in general, gave results that do not warrant its cost for computer implementation.

Smooth curves, coupled with good geologic information, could be substituted at a fraction of the cost.

RECOMMENDATIONS

Geophysical field data invariably requires correction and adjustment before any qualified judgment about geologic causes can be offered. This is particularly true in the case of gravity data.

The actual number of calculations for any given research or exploration project is variable. Automatic digital computation proved to be very helpful when applied to this project. It soon became apparent that the zest and intuitive feel for data and results was retained at a higher level simply because the results were obtained sooner with less tedious number manipulation.

Since the culmination of this report, it soon became apparent that computers are rapidly becoming an integral part of the petroleum and mining industry. It is strongly recommended that some method of digital computer programming be included in a student's elective curriculum. This will not only provide him with a powerful research tool, but will enhance his employment potential.

Specifically, in regard to this study, more research should be undertaken in the areas of approximation of regional gradients. The utilization of mathematical models and their application to geologic conditions should prove fruitful.

Some possible areas of research could include the following:

- 1. Fourier analysis,
- 2. Correlation studies,
- 3. Correlation between density and 2nd derivative values,
- 4. Variable density studies,
- 5. Automatic digital map contouring,
- 6. Spectral analysis,
- 7. Determination of 2nd derivative values from the derivative of the generating analytical function and comparison with an approximation function,
 - Application of the above mentioned methods to three-dimensional data,
 - More detailed investigation into upwards and downwards continuation systems,
 - 10. Development of new resolving methods for the analysis of potential field type geophysical data.
- Within any of these broad areas research might prove fruitful, and would increase the state of the art considerably.

BIBLIOGRAPHY

- Agocs, W. B., 1951, Least Squares Residual Anomaly Determination. Geophysics. vol. 16:686-696.
- Beutner, E. L., Characteristics of Some Iron Bearing Formations in Northern Wisconsin. Presented at Institute of Lake Superior Geology; Duluth, Minnesota.
- Brown, Jr., W. F., 1956, Minimum Variance in Gravity Analysis.

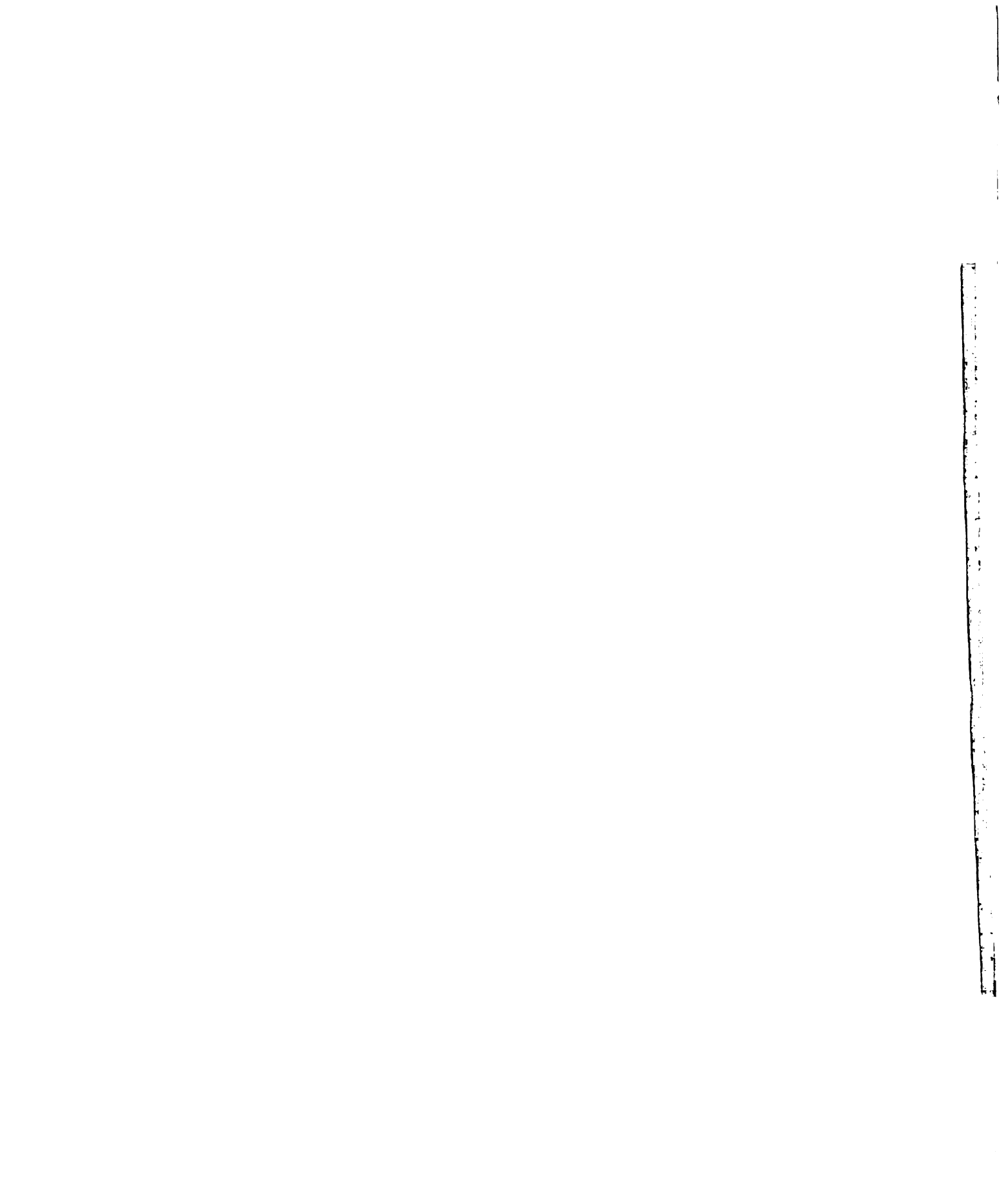
 Part II, Two-Dimensional. vol. XXI, no. 1:107-141.
- Brown Jr., W. F., 1955, Minimum Variance in Gravity Analysis.

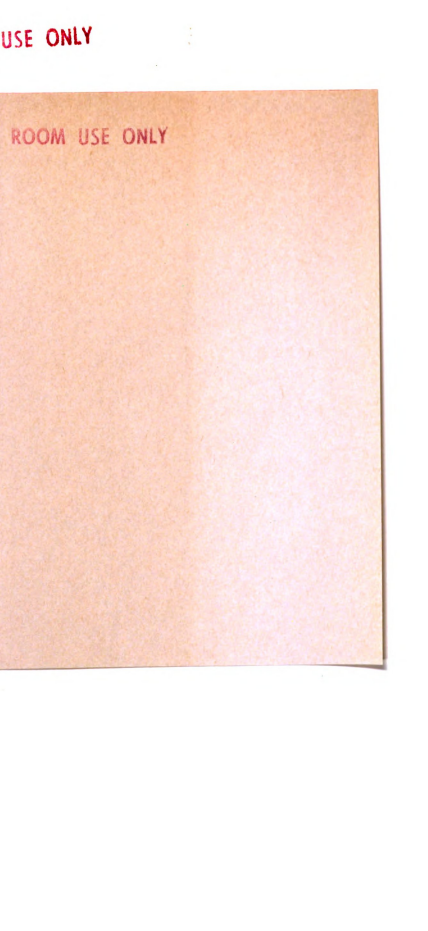
 Part I, One-Dimensional. vol. XX, no. 4:807-828.
- Bullard, E. L. and Cooper, R. I. B., 1948, The Determination of the Masses Necessary to Produce a Given Gravitational Field. Proc. Royal Society of London. vol. 194:332-347.
- Elkins, Thomas A., 1950, The Second Derivative Method of Gravity Interpretation. Geophysics. vol. XVI, Jan., no. 1:29-50.
- Gair, J. E. and Wier, R. L., 1956, Geology of Kiernan Quadrangle, Iron County, Michigan. U.S.G.S. Bulletin no. 1044.
- Grant, Fraser S., 1953, A Theory for the Regional Correction of Potential Field Data. Geophysics. vol. XIX, Jan. no. 1:23-45.
- Grant, F. G., 1957, A Problem in the Analysis of Geophysical Data. Geophysics. vol. 22, no. 3:309-344.
- Griffen, Raymond W., 1949, Residual Gravity in Theory and Practice. Geophysics. vol. XIV, Jan. no. 1:36-56.
- Heiland, C. A., 1940, Geophysical Exploration. Prentice-Hall, Inc. New York.
- Henderson, R. G. and Isadore Zietz, 1949, The Computation of the Second Vertical Derivatives of Geomagnetic Fields. Geophysics. vol. 14:508-534.
- Hinze, W. J., 1963, Personal Communication.

- Hinze, W. J., 1960, Application of the Gravity Method to Iron Ore Exploration. Economic Geology. vol. 55:465-484.
- Hubbert, 1948, Gravitational Terrain Effects of Two-Dimensional Topographic Features. Geophysics. vol. 13, no. 2:226.
- Jakosky, J. J., 1957, Exploration Geophysics. Trija Publishing Company. Newport Beach, California.
- Kaula, W. M., 1959, Statistical and Harmonic Analysis of Gravity.
 J. Geophysics Research. vol. 64, no. 12:2401-2421.
- Kraumbein, 1959, Trend Surface Analysis of Contour-Type Maps with Irregular Control-Point Spacing. J. Geophysics Research. vol. 64, no. 7:823-834.
- Mooney, Harold M. and Bleifuss, Rodney, 1953, Magnetic Susceptibility Measurements in Minnesota: Part II, Analysis of Field Results. Geophysics. vol. 18:383-393.
- Nettleton, L. L., 1940, Geophysical Prospecting for Oil. McGraw-Hill Book Company., Inc. New York.
- Nettleton, L. L., 1954, Regionals, Residuals and Structures. Geophysics. vol. XIX, Jan., no. 1:1-22.
- Peters, L. J., 1949, The Direct Approach to Magnetic Interpretation and its Practical Application. Geophysics. vol. XIV, July, no. 3:290-319.
- Saxov, Svend and Nygaard, Kurt, 1953, Residual Anomalies and Depth Estimation. Geophysics. vol. 13:913-928.
- Skeels, D. C., 1947, Ambiguity in Gravity Interpretation. Geophysics. vol. 12:43-56.
- Talwani, M., Worzel, Lamar J., and Landisman, Mark, 1959, Rapid Gravity Computations for Two-Dimensional Bodies With Application to the Mendocino Submarine Fracture Zone. J. Geophysics Research. vol. 64, no. 1:49-59.
- Talwani, M., 1960, Rapid Computation of Gravitational Attraction of Three-Dimensional Bodies of Arbitrary Shade. Geophysics. vol. XXV, no. 1:203-225.

- Trejo, Cesak A., 1954, A Note on Downward Continuation of Gravity. Geophysics. vol. XIX, Jan., no. 1:71-75.
- Vajik, Raoul, 1951, Regional Corrections of Gravity Data.

 Geofisica Pura E Applicata, Milano, Italy. vol. 19, Fasc, 3-4:143-219.
- Van Hise, V. R., Baley and Smyth, 1897, The Marquette Iron Bearing District of Michigan, Depth of Interior. U.S.G.S. monograph no. XXVIII.





Pocket has: 4 102 470 THS Plate 1 14 T P SUPPLEMENTARY

PLATE I
AMASA OVAL AREA

